Dissertationes Forestales 373

Remote sensing of surface fires in boreal forests

Noora Tienaho

School of Forest Sciences
Faculty of Science, Forestry and Technology
University of Eastern Finland

Academic dissertation

To be presented, with the permission of the Faculty of Science, Forestry and Technology of the University of Eastern Finland, for public criticism in Auditorium N100, University of Eastern Finland, Yliopistokatu 7, Joensuu, on the 19th of June 2025, at 1 pm.

Title of dissertation: Remote sensing of surface fires in boreal forests
Author: Noora Tienaho

Dissertationes Forestales 373
https://doi.org/10.14214/df.373

Thesis supervisors:
Docent Ninni Saarinen
School of Forest Sciences, University of Eastern Finland, Finland

Professor Mikko Vastaranta
School of Forest Sciences, University of Eastern Finland, Finland

Doctor Tuomas Yrttimaa
School of Forest Sciences, University of Eastern Finland, Finland

Pre-examiners:
Doctor Shaun Levick
Commonwealth Scientific and Industrial Research Organization, Land and Water, Australia

Doctor Andrew Hudak
Forestry Sciences Laboratory, United States Department of Agriculture, USA

Opponent:
Docent Inka Bohlin
Department of Forest Resource Management, Swedish University of Agricultural Sciences, Sweden

ISSN 1795-7389 (online)
ISBN 978-951-651-836-0 (pdf)

Publishers:
Finnish Society of Forest Science
Faculty of Agriculture and Forestry of the University of Helsinki
School of Forest Sciences of the University of Eastern Finland

Editorial Office:
Finnish Society of Forest Science
Viikinkaari 6, 00790 Helsinki, Finland
https://www.dissertationesforestales.fi

Tienaho N. (2025) Remote sensing of surface fires in boreal forests. Dissertationes Forestales 373. 50 p. https://doi.org/10.14214/df.373

ABSTRACT

Forest fires threaten carbon storage but are vital to boreal ecosystem dynamics. While crown fires are well-studied, low-intensity surface fires, common in Fennoscandia, are less understood. This thesis used remote sensing techniques to examine surface fires across eight Scots pine-dominated test sites (~1 ha each) in southern Finland, with controlled burnings simulating surface fires. Terrestrial laser scanning (TLS) reconstructed forest structure before and after these fires for change detection.

Study **I** utilized bitemporal TLS to identify burned areas and estimate volumetric changes in ground vegetation. A surface differencing-based classification method was developed, achieving high accuracy (recall, precision, F1-score = 0.9). On average, 85% of the test site areas were burned, with a mean reduction in ground vegetation volume of 1200 m^3/ha, though variability was observed.

Study **II** examined the effects of ground vegetation on TLS-derived digital terrain models (DTMs) and tree/forest attributes. In burned areas, post-fire DTMs averaged 10 cm lower than pre-fire DTMs, with greater changes and root mean square differences compared to unburned controls. A 10 cm overestimation in DTMs led to underestimates in tree/forest attributes: 1.3 mm (0.6%) in diameter at breast height, 4.8 dm^3 (3.1%) in stem volume, and ~3 m^3/ha (1.3%) in total stem volume.

Study **III** assessed the normalized burn ratio (NBR) index from Sentinel-2 data for detecting surface fires. Breakpoint analysis identified most fires, with undetected cases linked to sparser vegetation loss and denser canopy cover. A moderate negative correlation (r = –0.5) was found between NBR changes and TLS-derived volumetric changes in ground vegetation. Variations in NBR were explained by vegetation changes, canopy cover, and site conditions (R^2 = 84%).

This thesis demonstrates the potential of remote sensing to identify surface fires and quantify their effects on ground vegetation, supporting method development and advancing understanding of their role in boreal forest ecosystems.

Keywords: forest fires, terrestrial laser scanning, multispectral satellite imaging, Sentinel-2, burn severity, digital terrain model

ACKNOWLEDGEMENTS

In the summer of 2018, my life took a new direction. At the time, I was conducting research on the philosophy of electronic music, grounded in critical theory, but I found myself longing for something more tangible and down-to-earth. I began exploring new fields of study through a process of elimination: nothing related to culture, the humanities, or people, nor anything in the field of engineering sciences. Having recently inherited a small forest property and taken part in training sessions for new forest owners, the decision came quite naturally. I was already enrolled in musicology at the University of Helsinki, and in the autumn of 2018, I began attending forest science lectures under the open minor study rights. In Finnish, ‘music’ and ‘forest’ begin with the same letters. And fundamentally, everything is philosophy.

I adapted to forest studies very well and made wonderful friends – special thanks to Tiina and Jari-Pekka, with whom I still rant about forests and life in general. My heartfelt thanks also go to my former partner Markus, who made it possible for me to pursue my studies and provided open-minded, optimistic, and intellectually inspiring support. Towards the end of my studies, I saw that Ninni was seeking a thesis student for a remote sensing project. My original plan was to graduate quickly and move on to a concrete job outside academia. However, in one of the final thesis meetings, Mikko happened to be present – and together with Ninni, they lured me back into research. Looking back, it now feels inevitable, and I’m grateful to them both for their encouragement and belief in me.

I thus began my doctoral studies at the University of Eastern Finland, focusing on the remote sensing of forest fires. Fire and burning – topics close to my heart – reinforced my belief that I was on the right path. I was warmly welcomed into the scientific community and continuously received generous and helpful support. Special thanks go to Tuomas, who tirelessly assisted me in solving technical problems. I also wish to thank Eetu, Samantha, and Arttu for sharing their expertise in satellite data. I received valuable peer support from my fellow doctoral students in our research group – thank you, Reinis, Antti, Maryam, Ghasem, and Nivedhitha.

I wouldn’t have stayed sane without my family and friends. Thank you, mom and dad, for always (somewhat misguidedly) believing that I know what I’m doing – and for never holding me back. I’m deeply grateful to the many friends who have supported me and patiently listened to my overly enthusiastic explanations about forests. Special thanks to Hanne, Kaisa, Mari, and Matti. Above all, my greatest thanks go to my big sister Jenni. I wouldn’t be here without her. I followed her into the natural sciences (though not through the engineering path), and she has always been my biggest role model and dearest friend.

Tampere, May 2025

Noora Tienaho

LIST OF ORIGINAL ARTICLES

This thesis is based on the following research articles, referred to by the Roman numerals **I–III.** Articles **I** and **III** are reprinted with the permission of the publishers, while article **II** is the author's version of the submitted manuscript.

I Tienaho N, Saarinen N, Yrttimaa T, Kankare V, Vastaranta M (2024) Quantifying fire-induced changes in ground vegetation using bitemporal terrestrial laser scanning. Silva Fennica 58(3), article id 23061. https://doi.org/10.14214/sf.23061

II Tienaho N, Yrttimaa T, Saarinen N, Vaaja M, Vastaranta M (2025) Effects of ground vegetation on terrestrial laser scanning-derived digital terrain models in boreal forests. Unpublished manuscript.

III Tienaho N, Wittke S, Yrttimaa T, Kivimäki A, Puttonen E, Saarinen N & Vastaranta M (2025) Examining low-intensity surface fires in boreal forests using Sentinel-2 time series and bitemporal terrestrial laser scanning. Scandinavian Journal of Forest Research. https://doi.org/10.1080/02827581.2025.2457469

AUTHOR CONTRIBUTION

The articles were planned collaboratively with the supervisors. Tienaho collected terrestrial laser scanning (TLS) data with her colleagues and processed it with the assistance of Tuomas Yrttimaa. Satellite data for article **III** was collected and pre-processed by Samantha Wittke and Arttu Kivimäki. Tienaho was responsible for the analyses, calculations, model development, and accuracy evaluation in all sub-studies. As the main author, Tienaho wrote the initial drafts of all the manuscripts and led the review processes. The final versions of the articles were improved by the contributions of all co-authors.

TABLE OF CONTENT

ABBREVIATIONS

ΔDTM	change in digital terrain models
3D	three-dimensional
AIC	Akaike information criterion
ALS	airborne laser scanning
CBI	composite burn index
CHM	canopy height model
D_g	basal area-weighted mean diameter
DBH	diameter at breast height
DEM	digital elevation model
dNBR	difference normalized burn ratio
DSM	digital surface model
DTM	digital terrain model
FN	false negative
FP	false positive
G	basal area
GNSS	global navigation satellite system
h	tree height
H_g	basal area-weighted mean height
IMU	inertial measurement unit
lidar	light detection and ranging
N	number of stems
NBR	normalized burn ratio
NDVI	normalized difference vegetation index
NIR	near-infrared
OLI	operational land imager
r	correlation
R^2	coefficient of determination
radar	radio detection and ranging
RdNBR	relative difference normalized burn ratio
RMSD	root mean square difference
RMSE	root mean square error
RTX	real-time extended technology
SAR	synthetic aperture radar
SWIR	short-wave infrared
TIN	triangulated irregular network
TLS	terrestrial laser scanning
TP	true positive

1 INTRODUCTION

1.1 Fire in boreal forests

Each year, approximately 340–370 million hectares of the Earth's surface are affected by fire, though the actual burned area is likely higher due to technical limits and difficulties in detecting small fires, full time coverage, and cloud cover (FAO 2024). Forests, which serve as carbon sinks by absorbing carbon dioxide (CO_2) from the atmosphere, release stored carbon when they burn, contributing to greenhouse gas emissions and accelerating global warming (Szpakowski & Jensen 2019, Gajendiran et al. 2024). This creates a dangerous positive feedback loop, where climate change leads to warmer temperatures, drier conditions, and prolonged droughts, which in turn increase the frequency and intensity of wildfires (Flannigan et al. 2005, Keywood et al. 2013, Szpakowski & Jensen 2019). Additionally, forest fires cause habitat and ecosystem destruction, soil degradation, air pollution, and substantial economic losses in agriculture and forestry (Keywood et al. 2013, Gajendiran et al. 2024).

Boreal forests cover 27% of the global forest area, approximately 1 100 million hectares (FAO 2020). They span vast regions across North America and Eurasia, and are characterized by mild, short summers and cold winters. The growing season is relatively short, typically lasting 80 to 150 days (Saucier et al. 2015). The canopy layer is predominantly composed of coniferous species from the genera *Picea*, *Pinus*, *Abies*, and *Larix*, with deciduous trees from the genera *Betula*, *Populus*, *Alnus*, *Sorbus*, and *Salix* also present (Saucier et al. 2015). These trees are well-adapted to cold temperatures, nutrient-poor soils, and frequent stand-replacing disturbances (Saucier et al. 2015). The ground vegetation typically includes ericaceous dwarf shrubs such as *Vaccinium myrtillus* and *Vaccinium vitis-idaea*, feather mosses like *Pleurozium schreberi*, *Hylocomium splendens*, and *Ptilium crista-castrensis*, and herbaceous species suited to acidic soils, including *Deschampsia flexuosa*, *Luzula pilosa*, *Linnaea borealis*, and *Melampyrum pratense* (Palviainen et al. 2005, Saucier et al. 2015).

Despite their negative impacts, fires are a natural part of boreal forest dynamics. They create variability in forest age, structure, and composition, along with varying amounts of charred and decaying wood, which in turn provide habitats for diverse species (Parviainen 1996, Ryan 2002, Jonsson et al. 2005, Keywood et al. 2013). Fire particularly benefits pyrophilic and saproxylic species, such as certain insects and fungi, which are crucial for maintaining ecological balance in forest ecosystems (Penttilä et al. 2013, Bell 2023). Fires release nutrients back into the soil, reduce soil acidity, and provide optimal conditions for new seedlings to sprout and grow (Keeley & Fotheringham 2000, Laurila & Vierula 2020). By reducing fuel loads, fires can prevent larger, more destructive wildfires (Kreider et al. 2024). They also contribute to forest health, as the remaining vegetation tends to be stronger and more resilient. This resilience is further enhanced by increased biodiversity, which strengthens the forest's ability to recover from future disturbances (Thompson et al. 2009). Therefore, studying forest fires in boreal environments is essential for understanding both the ecological impacts and the resulting structural and functional changes.

While wildfires are becoming more frequent globally, their occurrence in Fennoscandian boreal forests has significantly decreased, largely due to intensive forestry practices, an extensive forest road network, and efficient fire detection and suppression systems (Vanha-Majamaa et al. 2004, Lindberg et al. 2018). Intensive forestry has reduced the amount of dry and dead wood, as well as other fuel loads in forests, and forest roads serve both as firebreaks and enable quick access for fire suppression (Kennedy et al. 2019). This decline in natural fires has increased the need for controlled burnings to maintain forest biodiversity. Controlled or prescribed burning – the deliberate use of fire for silvicultural and ecological management – serves multiple functions worldwide, such as reducing fuel loads to prevent larger fires, managing pests and diseases, and restoring ecosystems. In Fennoscandian forests, controlled burnings were historically used after final felling to facilitate reforestation (Karjalainen 1994, Lemberg & Puttonen 2002), but today they are primarily employed for ecological restoration.

Forest fires can be classified into crown, surface, and ground fires based on the type of fuel they consume (Lindberg et al. 2011, Greene & Michaletz 2015). Crown fires burn the forest canopy, surface fires primarily consume ground vegetation and detritus, while ground fires burn organic topsoil and roots near the surface in a slow, smoldering process (Greene & Michaletz 2015, Pérez-Izquierdo et al. 2020). In North America, severe stand-replacing crown fires are more common, whereas in the Fennoscandian region, wildfires are predominantly ground and surface fires (Päätalo 1998, Shorohova et al. 2011, Gauthier et al. 2015, Rogers et al. 2015). Surface fires typically consume shrub, herbaceous, and moss layers (Marozas et al. 2007, Buriánek et al. 2013), and may also affect understory trees and accumulated fuel loads, such as thinned trees left on the forest floor. Nowadays, controlled burnings in Fennoscandia are primarily designed to target forest floor vegetation while preventing the fire from reaching the canopy, thereby simulating the effects of natural surface fires.

Overall, monitoring and studying forest fires is essential due to their profound impacts on ecosystems, climate, and human health. A deeper understanding of fire behaviour enhances fire management and ecological restoration strategies, mitigates risks to communities and wildlife, and aids in assessing long-term effects on climate change and forest resilience.

1.2 Forest fire research: Field surveys and laboratory experiments

Forest fire research utilizes various methods, including field surveys, laboratory experiments, modelling, and remote sensing. Field measurements are used for tasks such as mapping burned areas, assessing burn severity, and monitoring post-fire recovery. Global navigation satellite systems (GNSS) can be employed to delineate fire-affected areas, but dense canopies may weaken signals, and rough terrain or remaining vegetation complicate data collection (Corona et al. 2008). Additionally, fires often burn in a patchy manner, complicating boundary definition, while large size of burned areas presents further challenges (Corona et al. 2008, Lazzeri et al. 2021). Burn severity is typically assessed in the field using the composite burn index (CBI), which provides a visual estimate of fire effects across five forest strata, combining these observations into a single index value (Szpakowski & Jensen 2019, Fassnacht et al. 2021, Gallagher et al. 2021). The five strata assessed are: 1) substrates, 2) herbs, low shrubs, and trees under 1 m, 3) tall shrubs and trees from 1–5 m, 4) intermediate trees, and 5) tall trees (Key & Benson 2006). However, the CBI tends to emphasize upper canopy effects, overlooking the forest floor, where surface fires have the greatest impact (Gallagher et al. 2021). Moreover, the CBI does not quantify the amount of burned vegetation, which is crucial for assessing climatic impacts. Monitoring vegetation recovery in the field can involve assessing seedling germination and regrowth (García-Morote et al. 2017). In addition to these challenges, field surveys face issues such as safety risks, limited accessibility, and significant time and labour demands (Gitas et al. 2012, Lazzeri et al. 2021).

Laboratory measurements are conducted to simulate fire behaviour and combustion processes, allowing for a detailed examination of how fire affects vegetation and soil in a controlled environment. Key metrics in these studies include heat release rate, which quantifies the energy released during combustion (Wang et al. 2023), particulate matter, which significantly impacts air quality (Hosseini et al. 2013), and fuel moisture content, a critical factor influencing ignition and burn characteristics (Rossa et al. 2016). To complement these experimental studies, mathematical and computational modelling techniques are employed to simulate fire behaviour (Cardil et al. 2021), predict fire spread (Ning et al. 2024), and assess the ecological impacts of fires (Or et al. 2023). Despite their value, both laboratory experiments and modelling approaches face limitations in accounting for all relevant environmental variables and the complex interactions between fire and atmospheric conditions (Ning et al. 2024).

1.3 Forest fire research: Remote sensing

1.3.1 Overview of remote sensing in forest fire research

Remote sensing addresses many of the above-mentioned limitations related to field surveys and laboratory experiments by providing extensive spatial and temporal coverage in a cost-effective manner, and by enabling a more comprehensive assessment of topographical, ecological, and climatic influences as it captures data under real-world conditions. Remote sensing plays a critical role in forest fire research across multiple domains, such as fire risk assessment, fuel mapping, active fire detection, burned area estimation, post-fire vegetation recovery monitoring, and burn severity estimation (Szpakowski & Jensen 2019).

Rapid advancements in technology have increased the availability of sensors, data, and processing capabilities (Szpakowski & Jensen 2019, Fernández-García et al. 2023a). Remote sensing platforms, including satellites, aircraft, drones, and ground stations, gather environmental data using either active or passive techniques. Passive sensors encompass both thermal and optical technologies. Thermal sensors, which detect infrared radiation, are widely used for various applications, such as monitoring urban heat islands (Kasniza Jumari et al. 2023), detecting wildfires (Hendel & Ross 2020), and observing volcanic activity (Corradino et al. 2024). A key advantage of thermal sensors is their ability to operate at night, although they are limited by their inability to penetrate cloud cover. Prominent instruments equipped with thermal sensors include Landsat (TIRS), MODIS, ASTER, VIIRS, and earlier systems like TIMS. Optical technologies, which are more widely used in forest fire research, are discussed in detail in subsequent sections.

Active remote sensing sensors generate electromagnetic radiation that they emit towards the monitored environment, capturing the back-scattered energy as observations. Techniques that utilize this approach include radar (radio detection and ranging), such as synthetic aperture radar (SAR), and lidar (light detection and ranging). Radar operates in the microwave spectrum and is unaffected by daylight or weather, making it highly effective for Earth monitoring. Its ability to penetrate vegetation, snow, and clouds enables diverse applications, such as environmental monitoring (Amitrano et al. 2021), disaster response (Kaku 2019), topographic mapping (Bürgmann et al. 2000), and snow and glacier studies (Tsang et al. 2022). Key radar satellites like Sentinel-1, Radarsat-2, and TerraSAR-X have been used for tasks such as mapping burned areas and estimating burn severity (Tanase et al. 2010, Goodenough et al. 2011, Hosseini & Lim 2023). Lidar technologies are discussed in detail in subsequent sections.

1.3.2 Multispectral satellite imaging

Optical remote sensing utilizes satellite or aerial sensors to capture data from the Earth's surface using optical wavelengths, primarily within the visible spectrum, near-infrared (NIR), shortwave infrared (SWIR), and infrared ranges (Zhu et al. 2017). Optical sensors are generally classified into three types: panchromatic sensors, which capture radiation across a broad wavelength range; multispectral sensors, which measure radiation in several discrete spectral bands; and hyperspectral sensors, which collect data across 10 to 100 narrow bands (Zhu et al. 2017).

Optical remote sensing provides detailed information applicable to a variety of fields, including land cover classification and large-scale environmental monitoring. In forest fire research, optical satellite data is extensively utilized for numerous tasks, including fire risk forecasting, fire detection, burned area mapping, biomass estimation, vegetation recovery monitoring, and burn severity assessment (Corona et al. 2008, Leblon et al. 2012, Zhao et al. 2023, Avetisyan et al. 2023).

Fire risk mapping using remote sensing assesses the likelihood of fire occurrence, while fuel mapping focuses on identifying the distribution and quantity of combustible materials (Szpakowski & Jensen 2019). Various indices, such as the fire weather index and live fuel moisture content, are utilized to assess fire risks and hazards (Yebra et al. 2013, Miller et al. 2024). Detecting active fires is critical for effective wildfire management and control efforts. Burned area estimation, typically conducted using satellite data, provides accurate spatial representations of fire extent and perimeter (Nolde et al. 2020). Understanding post-fire vegetation recovery is essential for assessing the long-term ecological impacts of fires. Remote sensing-based post-fire monitoring commonly utilizes image classification, vegetation indices, or spectral mixture analysis (Gitas et al. 2012, Szpakowski & Jensen 2019). Image classification categorises satellite data into land cover types such as forest, water, or burned areas. Vegetation indices assess plant health by analysing reflectance in different wavelengths of light, while spectral mixture analysis distinguishes between surface components like soil, ash, and vegetation, offering a more detailed view of post-fire landscapes.

Forest fire research frequently focuses on the NIR and SWIR regions (Gallagher et al. 2020), as these wavelengths are highly sensitive to changes in soil and vegetation reflectance caused by fire (López García & Caselles 1991, Plenious & Koutsias 2013). Fire-affected vegetation exhibits distinct responses in these wavelengths: NIR reflectance decreases, while SWIR reflectance increases (López García & Caselles 1991, Fassnacht et al. 2021, Gallagher et al. 2021). NIR wavelengths are sensitive to chlorophyll in living plants, and the presence of charcoal and ash reduces the reflectivity (Miller & Thode 2007, Ji et al. 2011, Zhao et al. 2023). In contrast, SWIR reflectance is influenced by moisture content in soil and vegetation, increasing as vegetation cover decreases.

A widely used spectral index derived from these wavelengths, the normalized burn ratio (NBR), is commonly applied to assess burn severity (Escuin et al. 2008, Veraverbeke et al. 2011, Mallinis et al. 2018, Kato et al. 2019). Burn severity refers to the extent of environmental damage caused by a fire, encompassing factors such as biomass loss, tree mortality, vegetation recovery, and impacts on soil (Lentile et al. 2006, Keeley 2009, Soverel et al. 2010, Fernández-García et al. 2023b). Burn severity is not a direct measurement, and results can vary depending on the specific context or ecosystem under study (Lentile et al. 2006, Fassnacht et al. 2021). Since fire alters the optical properties of vegetation and soil, burn severity can be estimated by analysing changes in reflectance across different regions of the electromagnetic spectrum (Leblon et al. 2012, Fassnacht et al. 2021). NBR has largely replaced the normalized difference vegetation index (NDVI) as the standard index for burn severity, as it is less sensitive to atmospheric scattering and phenological changes (Epting & Verbyla 2005, Escuin et al. 2008, Veraverbeke et al. 2011, Szpakowski & Jensen 2019, Zagalikis 2023).

NBR values are typically calculated for both pre- and post-fire conditions, with changes measured using the difference normalized burn ratio (dNBR) (Szpakowski & Jensen 2019). The dNBR quantifies the absolute change between these conditions, offering an estimate of burn severity but without accounting for pre-fire vegetation variability. In contrast, the relative difference normalized burn ratio (RdNBR) measures the relative change caused by fire (Miller & Thode 2007, Soverel et al. 2010, Fassnacht et al. 2021). Studies comparing the accuracy of dNBR and RdNBR in representing burn severity have produced mixed results, often influenced by local environmental conditions (Miller & Thode 2007, Soverel et al. 2010, Cai & Wang 2022, Avetisyan et al. 2023). Furthermore, the factors driving variability in these indices are not yet fully understood (Fassnacht et al. 2021).

Validating burn severity assessments from satellite imagery requires field measurements (French et al. 2008), with the CBI commonly used for this purpose. However, the CBI relies on visual interpretation, making it subjective and prone to human error. Initially developed to validate satellite-derived NBR values (Lentile et al. 2006), the CBI shows a strong correlation with NBR in the ecosystems where it was originated (Key & Benson 2006). Yet, this relationship varies across different ecosystems (French et al. 2008, Fassnacht et al. 2021).

The primary spaceborne optical platforms used for assessing burn severity are the Landsat series, managed by the United States Geological Survey, and the Sentinel-2 mission, operated by the European Space Agency. Both missions are dedicated to Earth observation and operate in sun-synchronous orbits, yet they differ in terms of spectral, spatial, and temporal resolutions. Optical satellite data from these platforms is collected exclusively during daylight and under favourable atmospheric conditions, such as clear skies. Importantly, imagery from both Landsat and Sentinel-2 is freely accessible, facilitating widespread use in research (Phiri et al. 2020, Wulder et al. 2022).

The Landsat program currently includes Landsat 8 and Landsat 9 satellites, launched in 2013 and 2021, respectively. These satellites provide multispectral data through the Operational Land Imager (OLI), capturing nine spectral bands with a spatial resolution of 30 m for most bands. In contrast, Sentinel-2 consists of two satellites, Sentinel-2A and Sentinel-2B, launched in 2015 and 2017, respectively. Sentinel-2 offers multispectral data across 13 spectral bands, with four bands (red, green, blue, and NIR) at a 10 m resolution, while the remaining bands have resolutions of 20 or 60 m. Sentinel-2 has a revisit time of two to three days for mid-latitude regions, while the combined revisit time for Landsat 8 and 9 is eight days.

Forest fires are extensively mapped using multispectral imaging, as it is well known that forest fires alter forest reflectance, leading to a decrease in NBR values (Escuin et al. 2008, French et al. 2008). However, this phenomenon has been less studied in the context of low-intensity surface fires. While satellite-based NBR values typically exhibit a notable correlation with changes in the upper canopy, they may not accurately reflect the effects of fire on the forest floor due to canopy occlusion (Hudak et al. 2007, Lentile et al. 2006). Additionally, the impact of fire-induced structural changes on the forest floor on burn severity estimates is not well understood.

1.3.3 Laser scanning

Laser scanning is an active remote sensing technology that employs lidar to measure distances and create three-dimensional (3D) representations of environments. Two primary principles are used for distance measurement: phase-shift and time-of-flight methods. In phase-shift scanners, a continuous laser wave is directed toward a target, and the distance is determined by analysing the phase difference between the emitted and received signals (Yoon et al. 2011). Such instruments provide wide coverage, dense point data, and fast data collection. Phase-shift scanners are especially suitable for detailed measurements at short distances, typically up to 100 meters (Dassot et al 2011). In contrast, time-of-flight scanners emit pulsed laser light and calculate the distance by measuring the time it takes for a pulse to travel to the object and return to the sensor. By utilizing the speed of light in the given medium, the time for each pulse to return to the sensor is converted into a precise distance measurement (Melin et al. 2017). When combined with a GNSS and an inertial measurement unit (IMU), which record the position and orientation of the sensor, these distance measurements can be converted into a 3D representation of the environment. The returning laser signals are assigned 3D coordinates (XYZ), each depicting the position of the reflective target, collectively forming a point could. These point clouds can then be utilized to quantify various structural attributes, such as vegetation height, canopy density, surface elevation, or building geometry.

Laser scanning systems are generally classified into two main types: full-waveform and discrete-return. Full-waveform systems capture the entire return signal from each laser pulse, allowing for more detailed analysis (Kim et al. 2012). In contrast, discrete-return systems record only specific points, typically 1–5 per pulse, resulting in a simpler dataset (Hilker et al. 2010). The laser wavelength impacts a system's ability to characterize objects (Rosette et al. 2012). Shorter wavelengths, like green light (~550 nm), are better suited for water penetration, while NIR wavelengths are highly reflective in healthy vegetation, enabling more pulse energy to scatter through the canopy and reach the ground (Mandlburger et al. 2013). A commonly used wavelength for vegetation analysis is 1064 nm, which falls within the NIR spectrum (Rosette et al. 2012). Longer wavelengths, such as 1550 nm, help differentiate plant components like leaves, stems, and bark (Douglas et al. 2015). Using multiple wavelengths can enhance classification accuracy, particularly for object identification (Zhu et al. 2017).

Laser scanning encompasses satellite-based, aerial, and terrestrial applications. While the core principles are similar between these applications, differences arise in the size of the laser footprint. In this context, the footprint refers to the area illuminated by a single laser pulse, which is influenced by the laser's divergence and the distance to the target (Rosette et al. 2012). Footprint size determines the level of detail in observations, ranging from tens of meters in satellite-based systems, to centimetres in airborne laser scanning (ALS) and down to millimetres in terrestrial laser scanning (TLS) (Rosette et al. 2012). Although TLS offers the smallest footprint and therefore the most precise measurements, it is limited to smaller spatial extents compared to ALS or satellite lidar.

In forest research, satellite lidar is essential for large-scale mapping of forest structures and biomass, providing data on canopy height, density, and vegetation cover over extensive area (Sun et al. 2020). This technology facilitates the monitoring of long-term forest dynamics, such as deforestation, reforestation, and the effects of climate change. While lidar operates at shorter wavelengths than radar, offering more precise surface measurements (Fouladinejad et al. 2019), it cannot penetrate clouds, though it is not dependent on daylight. Key satellite lidar systems include ICESat (2003–2009), ICESat-2 (2018 onwards), and GEDI (2019 onwards). Despite its potential, the relatively recent availability of satellite lidar has limited its widespread use in forest research. Furthermore, the GEDI mission, while optimized for studying forest structure, primarily focuses on tropical and subtropical forests, resulting in limited data coverage for boreal regions.

By utilizing laser scanning systems mounted on aircraft, ALS provides detailed data on forest structure across landscapes, particularly regarding tree height and crown dimensions

(Vauhkonen et al. 2014). Applications of ALS include forest inventory (Kauranne et al. 2017), a wide range of change detection tasks (Okyay et al. 2019), and tree species classification (Michałowska & Rapiński 2021). In the context of forest fire research, ALS has been used to assess burn severity (Montealegre et al. 2014), analyse vegetation recovery (Magnussen & Wulder 2012), map fuel loads (Cameron et al. 2022), quantify fuel consumption (McCarley et al. 2024), and examine the impacts of fire on tree growth (Sparks et al. 2023).

Small and portable TLS systems are designed for detailed reconstruction of trees and sample plots. They can be mounted on a static tripod, typically positioned 1–2 meters above ground level, or on a moving vehicle (Rosette et al. 2012). TLS offers millimetre-scale geometric accuracy in point cloud reconstruction (Liang et al. 2016), making it ideal for detecting small-scale changes in trees or, in the context of surface fires, in ground vegetation. However, TLS has a limited capacity to capture point cloud reconstructions only from objects directly visible to the scanner, with occlusion caused by vegetation being a primary challenge when applied in forest conditions (Abegg et al. 2017). This limitation can be mitigated by adopting a multi-scan approach, where point cloud data is captured from different locations to provide a more complete view.

In forest research, TLS has been applied in various areas, including forest inventories (Liang et al. 2016), ecological monitoring (Orwig et al. 2018), and biomass estimation (Calders et al. 2020). In the context of forest fires, TLS has proven particularly useful for quantifying vegetation structure (Penman et al. 2023) and fuel loads (Rowell et al. 2016, Wallace et al. 2016). Unlike airborne and satellite sensors that view the forest from above, TLS uses a hemispherical measurement geometry inside the forest, providing detailed insights into lower forest layers – such as tree stems, understory, and ground vegetation – making it especially valuable for assessing the effects of surface fires (Gallagher et al. 2021). As a result, TLS is emerging as a promising alternative to the CBI, offering a more consistent, repeatable, and objective method for burn severity assessment (Gallagher et al. 2021). While TLS has been extensively studied for estimating the aboveground biomass and volume of individual trees (Lin et al. 2010, Seidel et al. 2011, Yao et al. 2011, Moskal & Zheng 2012), its application in quantifying ground vegetation dynamics remains relatively unexplored.

One important application of point clouds in forest characterization is the creation of digital elevation models (DEMs), which represent surface elevation relative to a reference point, such as sea level. DEMs include digital terrain models (DTMs), which represent bare ground, and digital surface models (DSMs), which account for vegetation and buildings. Subtracting the DTM from the DSM results in a canopy height model (CHM), useful for analysing forest structure (Rai et al. 2024). The accuracy of DTMs is critical across applications where point cloud-based measurements are conducted relative to the ground level. Accurately determined DTMs are therefore crucial for determining structural attributes such as tree height, diameter at breast height (DBH), and basal area (Bohlin et al. 2012, Muir et al. 2017). These attributes are essential for forest inventories and management, as they also serve as the basis for estimating volume and biomass.

Both ALS and TLS are routinely used for ground surface characterization (Montealegre et al. 2015, Baltensweiler et al. 2017). ALS is preferred for large-scale mapping tasks, such as national elevation models, due to its broad coverage. In contrast, TLS offers higher-resolution elevation models for smaller areas, making it particularly useful in forest surveying. While ALS may struggle with canopy penetration due to its larger footprint and lower point density (Guarnieri et al. 2009), TLS can generate dense point clouds, with hundreds of ground points per square meter (Muir et al. 2017). However, the field of view in TLS results in longer optical paths through vegetation, potentially obscuring the ground surface compared to the nadir view provided by ALS (Coveney & Fotheringham 2011).

Studies have found that DTMs generated by both ALS and TLS tend to overestimate ground elevation (Hodgson & Bresnahan 2004, Hopkinson et al. 2005, Guarnieri et al. 2009, Fan et al. 2014, Baltensweiler et al. 2017, Jurjević et al. 2021).

TLS elevation errors arise from various factors, including displacements, scan co-registration, point cloud georeferencing, interpolation, and ground point classification (Su & Bork 2006, Coveney & Fotheringham 2011, Fan & Atkinson 2015, Moudrý et al. 2019, Nelson et al. 2022). However, studies indicate that the most significant error source is vegetation cover, as dense vegetation can block laser penetration, causing occlusion (Coveney & Fotheringham 2011, Fan et al. 2014, Baltensweiler et al. 2017). Despite this, the influence of different vegetation types on DTM accuracy remains poorly understood.

1.4 Objectives of the thesis

This thesis utilized remote sensing technologies, specifically TLS and multispectral satellite imaging, to investigate low-intensity surface fires in boreal forests. The study was conducted across eight Scots pine-dominated test sites, each approximately one hectare in size, located in southern Finland. All sites underwent controlled burning as part of ecological restoration, with TLS measurements collected before and after the fires for change detection. Additionally, multispectral time-series data from the Sentinel-2 satellite was used to complement the analysis. Three sub-studies were conducted within this experimental design, each focusing on specific objectives to address the research questions presented in **Table 1**.

The objective of study **I** was to use bitemporal TLS data to quantify changes in ground vegetation following low-intensity surface fires. Quantifying such changes is crucial for planning, evaluating, and monitoring forest management strategies, as well as for providing inputs for fire behaviour and effects models (Loudermilk et al. 2023). Accurate assessments of ground vegetation can improve predictions related to low-intensity surface fire behaviour and their impact on carbon balance. The first research question examined whether surface fire-induced changes could be detected using bitemporal TLS. A method for identifying burned areas was developed, its accuracy was tested, and maps of the fire-affected areas were created. The second research question addressed the magnitude of volumetric changes in ground vegetation due to the surface fires and how these changes varied within and between the test sites.

The study **II** aimed to understand how ground vegetation affects TLS-derived DTMs. The controlled burnings removed forest floor vegetation, providing an opportunity to examine the effects of ground vegetation on TLS-derived DTMs. DTM measurements were taken both before and after vegetation removal, enabling comparisons between burned and unburned areas. The TLS data helped distinguish these areas, allowing for direct comparisons of the DTMs in areas where ground vegetation obscured the ground returns and in those where it did not. The first research question in study **II** examined whether elevation values are higher when ground vegetation is included in the dataset used to generate the DTMs. The second question explored how the height of ground vegetation influenced the differences between burned and unburned areas. To contextualize the findings, the study also analysed how changes in elevation within the DTMs affected tree and forest characteristics, such as DBH, tree volume, and stand volume. To ensure that the observed differences were due to vegetation changes rather than geolocation errors, the change between pre- and post-fire DTMs (ΔDTM) and root mean square difference (RMSD) were analysed for both burned and control areas. It was hypothesized that burned areas would exhibit higher ΔDTM and RMSD values compared to unburned controls.

Table 1. Research question. TLS=terrestrial laser scanning, DTM=digital terrain model.

Sub-study	Question 1	Question 2
I	Can changes caused by surface fires be detected using bitemporal TLS?	What is the magnitude of these changes, and how does it vary within and between different areas?
II	Are elevation values higher when ground vegetation is included in the DTM dataset?	How does the height of ground vegetation affect the differences between burned and unburned areas?
III	Can surface fires be identified from multispectral satellite time series?	Is there a correlation between satellite-derived spectral change and TLS-derived structural change?

Study **III** incorporated multispectral imagery from the Sentinel-2 satellites. While the effectiveness of multispectral satellite imagery in detecting severe crown fires is well-established (Escuin et al. 2008, French et al. 2008), its ability to detect low-intensity surface fires remains underexplored. Consequently, the first research question evaluated the ability of the Sentinel-2 time series to identify low-intensity surface fires, based on the hypothesis that such fires induce a detectable decline in the NBR values, which could serve as a reliable indicator for future satellite-based detection. The second research question examined the relationship between the dNBR values and structural changes in the ground vegetation, assuming that higher burn severity estimates would correspond to a greater decrease in ground vegetation volume. The impact of canopy cover on this relationship was also considered, with a hypothesis that denser canopy cover may hinder the ability of satellite imagery to capture fine-scale changes on the forest floor.

2 MATERIAL AND METHODS

2.1 Study area

The study area for this thesis included eight test sites, each approximately one hectare in size, located in national parks or protected areas across southern Finland (**Figure 1**). Controlled burnings were conducted in these areas by Metsähallitus (a state-owned enterprise managing and protecting state-owned land and water areas) during the summers of 2021 and 2022 as part of ecological restoration efforts. Most of the burnings occurred in June and July, with two sites treated in August (**Table 2**). While the ideal period for controlled burnings typically falls between mid-May and Midsummer (Laurila & Vierula 2020), favourable weather conditions can extend the burning season into August (Perkiö et al. 2012).

All the test sites located in central or southern boreal zone and were dominated by Scots pine (*Pinus sylvestris*) (**Table 2**). The test sites also contained Norway spruce (*Picea abies*) and small amounts of silver birch (*Betula pendula*). Forest types included dry heath, sub-xeric heath, and mesic heath forests (*Calluna*, *Vaccinium*, and *Myrtillus* types according to Cajander’s (1926) categorization). The stand age ranged from 50 to 150 years. The ground vegetation consisted of species commonly found in Fennoscandian pine forests, including feather mosses (*Pleurozium schreberi*, *Hylocomium splendens*) and dwarf shrubs (*Vaccinium* *myrtillus*, *Vaccinium vitis-idaea)* (Palviainen et al. 2005). With a few exceptions, the test sites were thinned before the controlled burnings, resulting in logging residues on the forest floor.

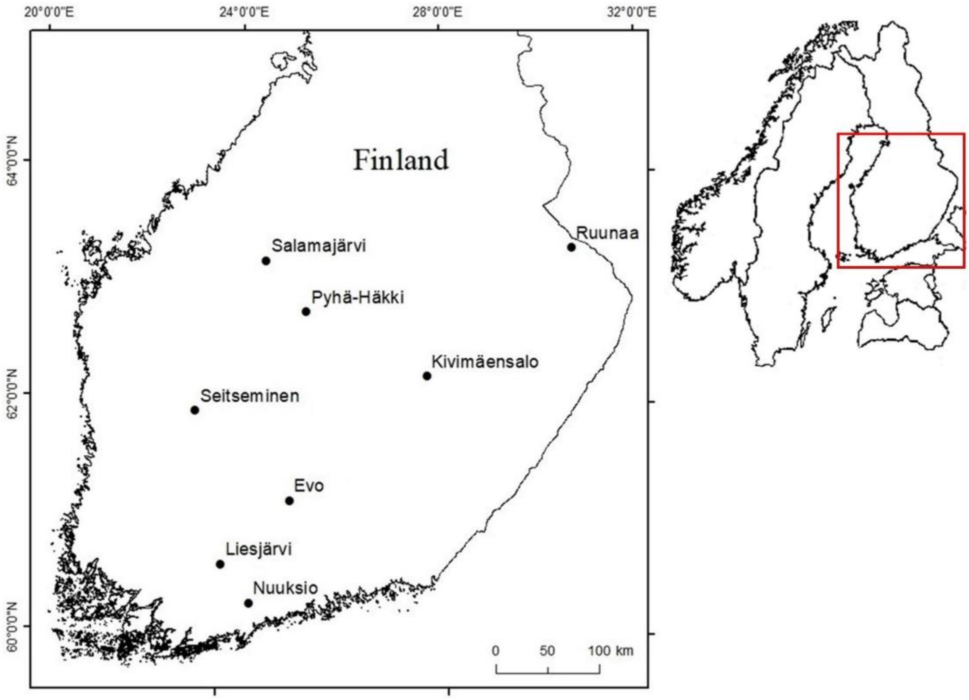

Figure 1. Eight test sites in southern Finland. Inset (right) adapted from the Europe blank political border map on Wikimedia Commons.

Table 2. Test sites in sub-studies, boreal subzone, forest type, stand age (~years), thinning information, dates of controlled burnings and pre- and post-fire terrestrial laser scanning (TLS) measurements. Stand age was provided by Metsähallitus.

Test site	Sub-study	Boreal subzone	Forest type	Age (~y)	Thin-ning	Pre-fire TLS, date	Burning date	Post-fire TLS, date
Kivimäensalo	I, III	southern	mesic heath	60	yes	10 Jun 2021	06 Jul 2021	09 Sep 2021
Liesjärvi	I, III	southern	sub-xeric heath	60	yes	16 Jun 2021	17 Jun 2021	05 Sep 2021
Pyhä-Häkki	I, III	central	sub-xeric heath	70	no	13 Jun 2021	30 Jun 2021	07 Sep 2021
Nuuksio	I, II, III	southern	sub-xeric heath	150	yes	06 Jun 2021	07 Jun 2021	30 Jun 2021
Seitseminen	I, II, III	central	sub-xeric heath	50	yes	20 Jun 2021	01 Jul 2021	06 Sep 2021
Evo	I, III	southern	mesic heath	60	yes	03 Jun 2022	15 Aug 2022	18 Aug 2022
Ruunaa	I, II	central	sub-xeric heath	120	no	09 Jun 2022	30 Jun 2022	03 Jul 2022
Salamajärvi	I, II, III	central	dry heath	70	no	13 Jul 2022	16 Aug 2022	13 Sep 2022

2.2 Terrestrial laser scanning data collection and processing

The TLS measurements were conducted on the test sites both before and after the controlled burnings. The time interval between pre- and post-fire measurements ranged from one to three months (**Table 2**). A multi-scan method was employed to ensure full point cloud coverage. This involved collecting multiple individual scans at a 10 × 10 m grid, resulting in approximately 120 scans per test site. The coordinates of the test site corners were measured using Trimble Geo 7X (Trimble Inc., Westminster, USA) equipped with real-time extended (RTX) GNSS positioning.

A Riegl VZ-400i time-of-flight laser scanner (RIEGL Laser Measurement Systems, Horn, Austria) was used to perform the TLS measurements. The scanner operates at a wavelength of 1550 nm and provides a 100° × 360° field of view with a beam divergence of 0.35 mrad. The 'Panorama 40' scan configuration was utilized, featuring a pulse repetition rate of 600 kHz, which enabled capturing up to eight returns per each emitted laser pulse. With these settings, the point spacing is 3.5 mm at a 10 m distance with an angular resolution of 0.04°. The pre- and post-fire scans for each test site were filtered and registered into a single merged point cloud using the RiSCAN PRO software (version 2.14.1) provided by the scanner manufacturer. The filtering process involved removing points with extreme reflectance values below –25 dB and above 5 dB. The scanner was equipped with integrated orientation and positioning sensors (i.e., IMU and GNSS receiver), which allowed for the registration of multiple scans without the need for artificial reference targets. Further processing of point clouds was conducted using LAStools software (version 211218) (Isenburg 2021).

The merged point clouds were first clipped with polygons based on the test site corner coordinates. To achieve precise alignment between the pre- and post-fire point clouds, the XYZ coordinates of tie points common to both measurements were manually extracted. These coordinates were then used to compute the necessary XYZ translation and XY rotation along the Z-axis, aligning the pre-fire point clouds with the post-fire ones. The XYZ translation was calculated as an arithmetic mean of the coordinate differences between the tie points. For the XY rotation, the angle and centre of rotation for each test site were identified by examining the intersections of bisectors of line segments connecting pairs of misaligned tie points (Ryan 2019). The alignments were visually inspected and further refined to achieve the closest possible match. Accuracy assessment showed a mean difference of 1–2 cm in all directions between the pre- and post-fire point clouds.

The point cloud coordinates were then rescaled to an accuracy of 1 mm to reduce the number of decimals and the overall data size. To eliminate noise from erroneous measurements, isolate points with fewer than six neighbouring points within a 2 cm radius were removed. Following this, the point clouds were voxelized into a 5 mm 3D grid to ensure a uniform point density and further reduce data size. Points were classified into ground and non-ground points following the procedure described in Ritter et al. (2017). Pre- and post-fire DTMs were subsequently generated by temporarily triangulating the ground points (originating from last or only returns) into a triangulated irregular network (TIN), which form a mesh of triangles connecting surface points. The TINs were then rasterized into DTMs using linear interpolation. The DTMs were produced at a 1 m resolution, a widely used standard in forestry applications. As the ground surface was expected to be more visible after the fire, the post-fire DTMs were used to normalize both the pre- and post-fire point clouds. The processing workflow is detailed in **Table 3**.

Table 3. Point cloud processing workflow.

Stage	LAStools	Settings
1) Clipping point clouds with polygons	lasclip	
2) Extracting tie points	lasview	
3) Translating and rotating pre-fire point clouds	las2las	-translate_xyz -rotate_xy
4) Rescaling the coordinates	las2las	-rescale 0.001 0.001 0.001
5) Removing noisy points	lasnoise	-step 0.02 -isolated 6 -remove noise
6) Thinning point clouds	lasvoxel	-step 0.005
7) Generating DTMs	lasground_new las2las las2dem	-step 1 -spike 0.4 -bulge 0.5 -offset 0.1 -keep_classification 2 -step 1 -last_only
8) Normalizing point clouds with post-fire DTMs	lasheight	-replace_z
9) Cutting point clouds to a height of 2 m	las2las	-keep_x -0.5 2
10) Generating vegetation surface models	lascanopy	-step 0.1 -p99

Table 4. Stand characteristics and mean elevation of the test sites. N=number of stems, G=basal area, D_g=basal area-weighted mean diameter at breast height, H_g=basal area-weighted mean height, Vol=stem volume, CC=canopy cover.

Test site	N (/ha)	G (m^2/ha)	D_g (cm)	H_g (m)	Vol (m^3/ha)	CC (%)	Elevation (m)
Kivimäensalo	732	17.1	18.7	16.9	140	54	164
Liesjärvi	527	12.7	19.2	16.1	93	42	140
Pyhä-Häkki	1 147	31.4	21.7	18.3	261	79	176
Nuuksio	369	21.2	31.0	20.6	205	55	100
Seitseminen	687	25.3	24.3	21.6	260	55	184
Evo	751	23.7	26.3	18.6	210	68	171
Ruunaa	948	28.5	21.5	19.6	274	76	152
Salamajärvi	919	30.7	23.0	19.6	272	65	190

Stand characteristics for each test site (**Table 4**) were derived from the pre-fire TLS point clouds using computational methods presented in Yrttimaa et al. (2019, 2020) and available in Yrttimaa (2021). These methods involved automatic tree detection, the separation of stem points from non-stem points, and the computation of single tree attributes, which were then used to derive the stand characteristics for each test site. The analysis was conducted using MATLAB (version R2023a). The stand characteristics included the number of stems, basal area, basal area-weighted mean diameter at breast height, basal area-weighted mean height, stem volume, and canopy cover. Canopy cover was calculated by first creating a boundary polygon for points associated with each tree, representing crown projection area on an XY plane, and then computing the ratio of their combined area to the test site area. Elevation data was derived from the post-fire DTMs.

As the controlled burnings only affected the ground vegetation, points located more than 2 m above the ground surface were omitted from further analyses (**Table 3**). Vegetation surface models for both the pre- and post-fire point clouds were generated on a two-dimensional grid with a resolution of 0.1 m, where each cell represented vegetation height (**Table 3**). The 99th height percentile was used to create the vegetation surface model instead of the maximum height to avoid noise and inaccuracies caused by extreme points (Friedli et al. 2016, Malambo et al. 2018). Despite the dense scanning setup, vegetation, topography, and obstacles like rocks inevitably caused some degree of occlusion. To fill in the missing values for cells with no point returns, the pre- and post-fire vegetation surface models were interpolated using the mean value of the nearest 9 × 9 cells. As a result of the TLS data processing, the height of the ground vegetation was determined for each 0.1 × 0.1 m cell, both pre- and post-fire.

2.3 Satellite data collection and processing

Sentinel-2 L2A (bottom of atmosphere) data for the test sites was downloaded from the ESA SciHub. The dataset spanned the summer months (May–August) of both the fire year and the five years prior. Given the small size of the test sites (1 ha), data was extracted from Sentinel-2 tiles (1 000 000 ha) with up to 95% cloud cover, as even heavily clouded scenes could contain clear pixels over the site. Cloud-related and defective pixels, as identified in the scene classification provided by the L2A product, were masked out. For the fire year, all data was visually inspected to ensure it was cloud-free at the test sites using true-colour images. For the five preceding years, true-colour images were reviewed whenever anomalies were detected in the derived values. Data from the cloud-covered dates was excluded from further processing. The EODIE toolkit (Wittke et al. 2023) was used for preprocessing the data.

The burn severity indices were calculated by using the NIR and SWIR bands, with central wavelengths of 842 nm and 2190 nm, respectively. The original pixel sizes for the NIR and SWIR bands were 10 m and 20 m, respectively, and both were resampled to a uniform 10 m pixel size. The NBR and dNBR values were then computed for each pixel at the test sites (n = 600) across all available dates, using the following equations:

$$NBR = \frac{NIR - SWIR}{NIR + SWIR} \tag{1}$$

$$dNBR = preNBR - postNBR \tag{2}$$

where NBR refers to normalized burn ratio, NIR to near infrared band, SWIR to short-wave infrared band, dNBR to difference normalized burn ratio, preNBR to NBR values before the fire, and postNBR to NBR values after the fire.

The study also examined RdNBR, but since a strong correlation was found between dNBR and RdNBR (> 0.95 for each test site), only dNBR values are reported in the results. The NBR produces values ranging from –1 to 1 with positive values indicating healthy, dense vegetation, and negative values suggesting recently burned areas (Escuin et al. 2008, Cai & Wang 2022). In contrast, the dNBR ranges from –2 to 2 with positive values reflecting high burn severity and negative values indicating increased vegetation cover (Miller & Thode 2007, Cai & Wang 2022).

In previous studies, a single satellite image closest in time to the comparative measurements has typically been used (e.g., Fassnacht et al. 2021). However, in this study, the TLS measurements were conducted at some test sites up to eleven weeks before or after the controlled burnings. Consequently, the pre- and post-fire NBR values for each cell were calculated by averaging the NBR values from the month preceding and the month following the fire. The number of cloud-free acquisitions within this period varied by test site, ranging from 2 to 9 before the fire and 2 to 7 after the fire.

2.4 Identifying burned areas and quantifying the volume of burned vegetation (I)

In study **I**, the TLS-derived vegetation height models were utilized to identify burned areas and to estimate volumetric changes in the ground vegetation. In this study, all eight test sites were included. It was assumed that a reduction in vegetation height indicated burned vegetation, while an increase or stability in height indicated unburned vegetation. Changes in ground vegetation height were estimated through surface differencing, which involved subtracting the pre-fire surface models from post-fire surface models. As a result of surface differencing, negative values indicated a fire-induced decrease in vegetation height, while positive values indicated a growth-induced increase.

The detailed surface models of changes in ground vegetation height were then aggregated into 1 × 1 m cells to provide a more concise view of the changes and to reduce noise from small-scale variation. These cells were then assigned a classification ’burned’ if more than half of the associated 0.1 × 0.1 m cells in each 1 × 1 m cell indicated a negative change. Otherwise, the cell was classified as ’unburned’. This classification allowed for the assessment of burn severity based on the proportion of the total test site area that was consumed by the fire.

The performance of the classification method was evaluated by randomly sampling 20 ‘burned’ and 20 ‘unburned’ cells from each test site and visually inspecting the associated point clouds. Overlaid pre- and post-fire point clouds from these cells were analysed, with a cell confirmed to have ‘burned’ if most pre-fire points appeared higher than those post-fire. Classification accuracy was assessed using recall, precision, and F1-score. The recall measures the proportion of true positives identified by the method versus the total true positives from visual inspection. The precision measures the proportion of true positives among all identified positives. The F1-score combines precision and recall into a single metric for comprehensive performance evaluation. In this context, true positives were those 1 × 1 m cells that were classified as ‘burned’ by both the TLS measurements and the visual inspection. False positives were cells incorrectly classified as ‘burned’, while true negatives were correctly identified as ‘unburned’, and false negatives were incorrectly classified as ‘unburned’. The accuracy measures were calculated with equations:

$$Recall = \frac{TP}{TP + FN} \tag{3}$$

$$Precision = \frac{TP}{TP + FP} \tag{4}$$

$$F1 = 2 \times \frac{Precision \times Recall}{Precision + Recall} \tag{5}$$

where TP refers to the number of true positives, FN to the number of false negatives, and FP to the number of false positives.

To estimate the volumetric extent of ground vegetation, the pre- and post-fire vegetation surface models at a 0.1 m resolution were used. The volume for each cell was calculated by multiplying the cell area by its associated vegetation height value, and the total volume was obtained by summing up these values for both time points. During the generation of surface models, all points below 2 m in height were included, resulting in the pre- and post-fire volumes accounting for not only ground vegetation but also tree stems. The change in this volume was determined by subtracting the pre-fire volume from the post-fire volume, with the contribution of tree stems eliminated as they remained stationary between the data captures. The observed changes, encompassing both fire-induced decreases and growth-related increases in vegetation height, were analysed separately at 0.1 m resolution. Variations in volume changes within the test sites were assessed using 1 × 1 m cells classified as either 'burned' or 'unburned', and the distributions of these changes were visualized using Tukey's boxplots.

2.5 Effect of ground vegetation on digital terrain models (II)

In study **II**, the TLS-derived vegetation height models were utilized to evaluate the effect of ground vegetation on DTM accuracy. Four test sites were used in this research: Nuuksio, Seitseminen, Ruunaa, and Salamajärvi. At these test sites, the alignment accuracy between pre- and post-fire point clouds showed a mean difference of 1.5 cm in the XY-plane and 1.2 cm in the Z-direction, with corresponding root mean square errors (RMSEs) of 7.5 cm and 3.2 cm, respectively.

It was hypothesized that the post-fire DTMs would characterize ground elevation at lower levels than the pre-fire DTMs due to the increased visibility of the ground surface following the removal of ground vegetation by the fire. Following the methodology outlined in study **I**, the 1 × 1 m cells representing changes in ground vegetation height were also classified based on the respective 0.1 × 0.1 m cells. However, the classification criteria were slightly adjusted as the analysis on DTM accuracy was targeted on cells with ground vegetation removed by the fire and cells where the vegetation had remained as intact as possible. A 1 × 1 m cell was classified as 'burned' if ≥ 80% of the 0.1 × 0.1 m cells exhibited a height decrease of > 5 cm, while it was classified as 'control' if ≥ 50% of the associated 0.1 × 0.1 m cells showed an absolute height change of ≤ 5 cm. The 5-cm height threshold was selected based on the evaluation of pre- and post-fire point cloud alignment, ensuring it surpassed the 3.2-cm RMSE achieved for the Z-coordinate accuracy. Cells that did not meet these criteria were excluded from further analysis. Based on this classification, the burned areas ranged from 3% to 60%, while control areas covered 10% to 25% of the total area of the test sites. Overall, the burned areas across all test sites totalled 1.2 ha, and the control areas covered 0.8 ha.

To assess the effects of ground vegetation on TLS-derived DTMs, ΔDTM was analysed separately for burned and control cells. This comparison ensured that any observed deviation between pre- and post-fire DTMs was due to the presence of vegetation in the pre-fire point clouds and its absence in the post-fire point clouds, rather than measurement errors or co-registration issues. The analysis focused on ΔDTMs and RMSDs between the pre- and post-fire DTMs. ΔDTMs were calculated by subtracting the pre-fire DTMs from the post-fire DTMs, and the mean ΔDTMs for burned and control areas were compared using Welch's two-sample t-test. The null hypothesis, assuming no difference between the means, was rejected if the p-value was ≤ 0.05.

While DTM accuracy is typically assessed by comparing it to a higher-accuracy validation dataset (e.g., points from a total station or differential global positioning system) and calculating RMSEs (Guarnieri et al. 2009, Fan & Atkinson 2015, Muir et al. 2017), study **II** did not include such validation. Instead, the focus was on evaluating the differences between bitemporal DTM measurements, with vegetation removal occurring in between. This approach allowed for a direct assessment of vegetation effects using RMSD rather than RMSE. While RMSE measures the difference between predicted and actual values, RMSD quantifies the difference between two sets of observed data. The equation for RMSD is as follows:

$$RMSD = \sqrt{\frac{\sum_{i=1}^{n}(preDTMi - postDTMi)^2}{n}} \tag{6}$$

where RMSD = root mean square difference, *pre*DTM = pre-fire DTM, *post*DTM = post-fire DTM, and *n* = the number of observations.

To assess the effect of vegetation height on DTM accuracy, burned 1 x 1 m cells were categorized into three classes based on their mean pre-fire vegetation height: ≤15 cm, 15–30 cm, and >30 cm. The number of cells in each class was 1105, 6393, and 4951, respectively. ΔDTM was calculated for each class. The first class represents areas dominated by mosses and lichens, the second by common heather and lingonberry twigs, and the third by more fertile sites with bilberry twigs and various grasses, which resulted in higher vegetation heights.

Next, to evaluate the impact of DTM inaccuracies on forest characterization, the effect of ground height overestimation on diameter at breast height (DBH) and stem volume measurements was examined. Trees within the study sites were first identified in the post-fire TLS point clouds, and their stem taper curves were measured using automated processing tools from Yrttimaa et al. (2019, 2020). DBH was defined at 1.3 m based on the stem taper curves. The stem was modelled as a series of vertical cylinders, and volume was calculated for each 1-cm section using the cylinder volume formula. The total stem volume was obtained by summing the volumes of all sections. The sampled trees had an average DBH of 23.6 cm (range: 4.9–69.3 cm) and an average stem volume of 222.7 dm3 (range: 8.9–1701.0 dm3). Stand density (trees per hectare) was calculated by dividing the number of trees detected in the point clouds by the area of the study site. Total stem volume per hectare was obtained by summing the volumes of the detected trees and dividing by the same area. The results for the study sites were: 369 trees/ha and 205 m^3/ha for Nuuksio, 687 trees/ha and 260 m^3/ha for Seitseminen, 948 trees/ha and 274 m^3/ha for Ruunaa, and 919 trees/ha and 272 m^3/ha for Salamajärvi.

To further understand the impact of height offset on DBH measurements, a total of 100 trees were randomly sampled from each study site (n = 400 trees in total). For each tree, DBH was measured with a height offset of 0–30 cm from the actual measurement height of 1.3 m. This involved measuring stem diameter from post-fire taper curves at 1-cm intervals between 1.30 m and 1.60 m, with 1.30 m representing the correct height (0 cm offset) and 1.60 m representing the scenario where the ground level is overestimated by 30 cm, leading to a 30 cm higher DBH measurement. For each offset, the medium and 99% confidence intervals of diameter deviation from the true value were calculated.

To assess the impact of DTM inaccuracy on stem volume estimation, the focus was on the lower part of the stem, which may be omitted if the DTM overestimates due to ground vegetation. Using the taper curve, stem volume was calculated for cylinders with height offsets of 0–30 cm. The actual stem volume was first calculated from the base to the top of the tree, then volumes were recalculated for sections from 1 cm to 30 cm above the base, moving upward by 1 cm at a time. This approach allowed evaluation of how ground vegetation affects stem volume. Medium and 99% confidence intervals were computed for each height offset to quantify the volume of stem sections omitted due to DTM inaccuracy.

Finally, to understand how uncertainties in DTM estimation affect stand-level forest characterization, the impact of height offsets in stem volume estimation on total stem volume was calculated. The potentially omitted stem volumes of the sampled trees within each site (i.e., volume per 100 sample trees) were summed. These values were then scaled by the known stand density (trees per hectare) to estimate the omitted volume per hectare due to DTM inaccuracies.

2.6 Identifying surface fires via satellites and associations with TLS (III)

In study **III**, the ability to identify low-intensity surface fires from Sentinel-2 data was assessed by analysing the changes in forest reflectance during the fire year. This study focused on seven test sites (excluding Ruunaa), where sufficient satellite data were available. It was hypothesized that surface fires would lead to a significant drop in NBR values. To identify this change, a breakpoint analysis was performed. The NBR changes detected were then compared to the actual fire dates, with the temporal alignment providing quantitative evidence that surface fires can be identified through Sentinel-2 time series data. Daily NBR values from May 1 to August 31 of the fire year were estimated using cloud-free observations for each 10 x 10 m cell within the test sites, and a site-specific mean was calculated. Gaps between observation dates were filled and values beyond the last observation were extended using a Gaussian 30-day moving average smoothing and linear interpolation.

To ensure that any decline in the NBR values was due to surface fires rather than seasonal variation, a moving average of NBR values from the five years before the fire year was calculated and subtracted from the daily NBR estimates. This process yielded trend-removed NBR values. These adjusted values were then analysed for abrupt changes to identify signal change points, which were interpreted as indications of spectral changes in the test sites, suggesting fire events. The signal change point was determined by averaging three change points for each test site. The first two change points were identified using MATLAB's *findchangepts* function, which detected shifts in the mean and slope of both daily and trend-removed NBR estimates. The third change point was found by locating the minimum value of the 1st derivative of the trend-removed daily NBR estimates (representing the steepest negative slope). For each test site, the fire year's NBR values, the average from the preceding years, and the breakpoint analysis results were plotted together on the same graph.

It was hypothesized that higher burn severity values from Sentinel-2 data would align with greater reductions in TLS-derived ground vegetation volume. The volumetric changes in ground vegetation, initially calculated at 0.1 m resolution, were aggregated to match the 10 m resolution of the satellite imagery. Pearson's correlation coefficient and the coefficient of determination (R^2) were calculated between dNBR values and volumetric changes, and the results were visualized using scatter plots.

To identify factors influencing this relationship, the cells (n = 600) were first classified into four equal-sized groups (n = 150) based on the TLS-measured volume change: unburned, low burn, medium burn, and high burn. Volume change in the unburned group ranged from –6 to 32 m³, while the low, medium, and high burn groups showed volume decreases of 6–13, 13–21, and 21–47 m³, respectively. To assess how canopy cover affects this relationship, the dNBR values were analysed across these volume change groups under different levels of canopy cover. The 10 × 10 m cells were classified into three equal-sized groups (*n* = 200), representing low (≤ 54%), moderate (54–72%), and high (> 72%) canopy coverage. The mean dNBR values were examined within these groups, with results visualized using boxplots.

To assess how volumetric changes in ground vegetation, both alone and combined with canopy cover, affect dNBR values, two types of linear regression models were created, with dNBR as the response variable: 1) volume change as the sole fixed predictor, and 2) both volume change and canopy cover as fixed predictors. Additionally, mixed-effects models were used to examine the impact of ground vegetation volume and canopy cover changes on dNBR values, including the test site as a random effect to account for site-specific influences. Model performance was evaluated using the R^2 and the Akaike information criterion (AIC).

3 RESULTS AND DISCUSSION

3.1 Identifying burned and unburned areas

The classification method developed in study **I** for identifying ‘burned’ and ‘unburned’ areas by comparing the TLS-derived pre- and post-fire surfaces models proved effective. Out of the 320 1 × 1 m cells inspected for classification accuracy, 160 were classified as ’burned’ and 160 as ’unburned’ using the presented method. Visual inspection of these cells confirmed a correct classification assigned for 89% of the ’burned’ cells and 89% of the ’unburned’ cells. This resulted in an overall precision of 0.89, implying a high user’s accuracy. Out of the 160 cells that actually burned based on the visual inspection of the point clouds, 90% were correctly identified as ‘burned’ by the proposed method as well. This resulted in an overall recall of 0.90, indicating a high producer’s accuracy. Altogether, the F1-score combining both the recall and precision showed an overall accuracy of 0.88. The accuracy assessed through the F1-score varied slightly (from 0.74 to 0.98) across the test sites (**Table 5A)**. The proportion of the cells classified as ‘burned’ was 51–96%, depending on the test site, and the proportion of the ‘unburned’ cells was 4–49% (**Table 5B**). Maps of the fire-exposed areas are presented in **Figure 2**.

Table 5. **A)** Recall, precision, and F1-score quantifying the performance of the classification method for identifying ‘burned’ and ‘unburned’ areas. **B)** Proportions of ‘burned’ and ‘unburned’ 1 × 1 m cells for each test site.

	A) Classification accuracy			**B) Proportion of cells (%)**	
Site	Recall	Precision	F1-score	‘Burned’	‘Unburned’
Kivimäensalo	0.95	1.00	0.98	95	5
Liesjärvi	0.77	1.00	0.87	95	5
Pyhä-Häkki	0.95	0.95	0.95	92	8
Nuuksio	0.94	0.80	0.86	83	17
Seitseminen	0.80	1.00	0.89	94	6
Evo	0.87	0.65	0.74	51	49
Ruunaa	0.95	0.95	0.95	96	4
Salamajärvi	0.94	0.75	0.83	71	29
Mean	**0.90**	**0.89**	**0.88**	**85**	**15**

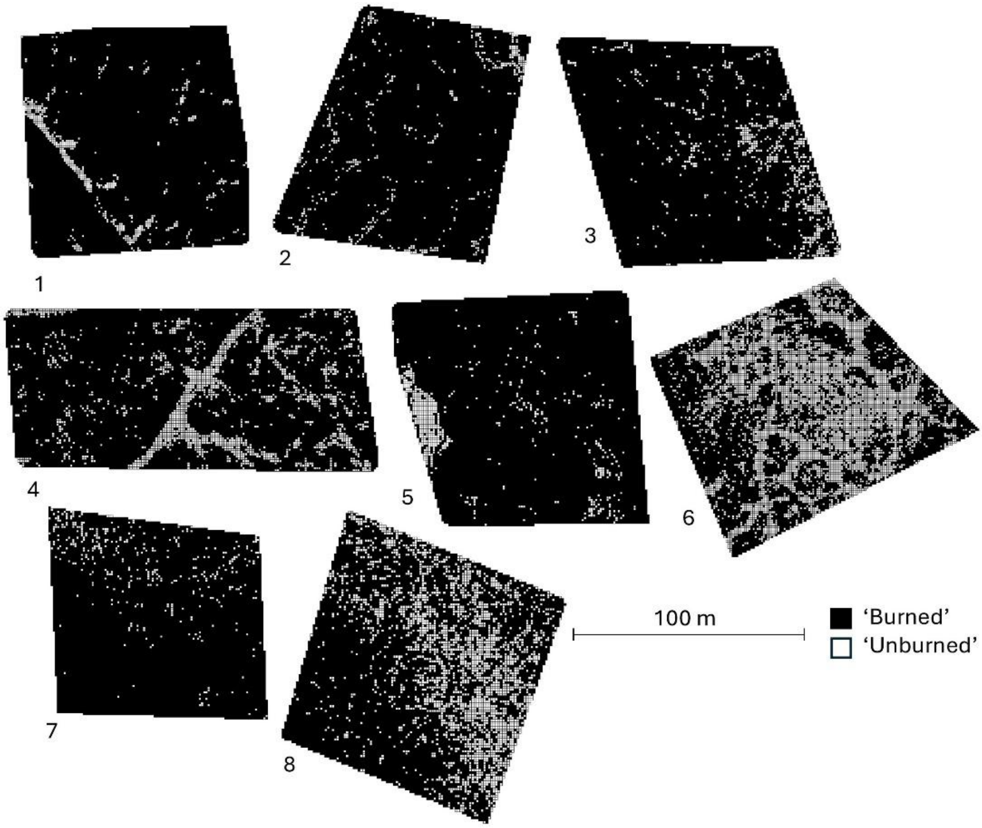

Figure 2. The spatial distribution of 1 × 1 m cells classified as 'burned' (black) and 'unburned' (white) in the north-south oriented test sites. 1 = Kivimäensalo, 2 = Liesjärvi, 3 = Pyhä-Häkki, 4 = Nuuksio, 5 = Seitseminen, 6 = Evo, 7 = Ruunaa, 8 = Salamajärvi.

The maps of the fire-exposed areas of this study were consistent with previous studies, showing that controlled burnings create a mosaic of burned and unburned areas (Penman et al. 2007, Perkiö et al. 2012, Loudermilk et al. 2023). For instance, controlled burnings in sclerophyll eucalypt forests affected about 60–70% of the area (Gupta et al. 2015). This uneven fire distribution is ecologically beneficial in many biomes, as it promotes habitat diversity through varying structures and functions. The observed variability in burn patterns is driven by complex forest conditions, such as differences in topography, fuel distribution, and interactions between fire and weather. The results of this study demonstrate that the bitemporal TLS was able to capture these variations.

Fire behaviour during controlled burnings is also influenced by practical factors such as ignition, control, extinguishing, and timing (Lemberg & Puttonen 2002, Laurila & Vierula 2020). To prevent fire spread beyond target areas, extensive watering is often applied before, during, and after the burning. Target areas are typically bordered by firebreaks (5–25 m wide, cleared of trees and combustibles) or fire lines (narrow strips of exposed mineral soil) (Lindberg et al. 2011, Perkiö et al. 2012, Laurila & Vierula 2020). These barriers remain unburned through watering or soil exposure. The impact of these artificial barriers as well as the practical factors were not assessed in this study, as it would have required continuous monitoring during the fire, which was beyond the scope.

3.2 Variability in the magnitude of fire-induced changes in ground vegetation

Study **I** utilized bitemporal TLS measurements also to estimate the extent and variation in the volumetric changes in the ground vegetation across the test sites. On average, the total change was –1 200 m^3/ha, with burning reducing it by 1 700 m^3/ha and vegetation growth increasing it by 500 m^3/ha. However, substantial variations in the volume changes were observed between the test sites (**Figure 3A**). The total volumetric changes ranged from –2 420 to 30 m^3/ha, with fire-induced reductions ranging from –2 640 to –980 m^3/ha, and growth-related increases ranging from 120 to 1 680 m^3/ha. Variations in the extent of pre-fire ground vegetation (**Figure 3B**) may have influenced the observed differences by affecting fuel availability. Substantial variation was also observed within the test sites when analysing cell-level changes (**Figure 4**). The 'burned' cells exhibited standard deviations of 0.10–0.22 m^3, while the respective range for the 'unburned' cells was 0.07–0.23 m^3.

Variations in the extent of these fire-induced changes can be partly explained by the site characteristics, such as the number and size of trees, which affect light and nutrient availability through competition, as well as soil moisture levels and the accumulation of leaf litter (Xiong & Nilsson 1999, Ludwig et al. 2004). These factors affect both the quantity and quality of ground vegetation and fuel load. For instance, the Kivimäensalo and Evo sites, that were characterized by a more nutrient-rich forest type (**Table 2**), exhibited considerable internal variability in the volumetric changes among both 'burned' and 'unburned' cells (**Figure 4**).

At Salamajärvi, the ground vegetation volume decreased only slightly (154 m^3/ha), while at Evo, it increased (33 m^3/ha) (**Figure 3B**). This could be due to the longer time gap between the pre-fire TLS measurements and the burnings compared to other test sites (**Table 2**). Additionally, the burnings at Evo and Salamajärvi took place in August, representing a suboptimal timing outside the preferred time window from mid-May to late June (Laurila & Vierula 2020), which may further explain these anomalies.

The Evo test site stands out from the other controlled burning sites in several ways. It had the largest unburned area (**Table 5**) and was the only site where ground vegetation volume increased (**Figure 3A**). The Evo test site also represented the highest extent in pre- and post-fire vegetation (**Figure 3B**), with the largest standard deviations in the observed volumetric changes, indicating more inconsistent fire impacts.

The unique fire behaviour observed at the Evo test site highlights the substantial variability in fire-induced biomass changes among the test sites as documented in other studies as well. For instance, Loudermilk et al. (2023) reported a mean biomass consumption of 580 g/m^2 with a standard deviation of 353 g/m^2 following controlled burnings in temperate coniferous forests. The large standard deviation emphasizes the importance of considering variations beyond stand-level averages. Relying solely on data from a single area may lead to misleading conclusions. In contrast, analysing changes across multiple controlled burning sites offers a more comprehensive understanding of variability and patterns in fire behaviour. This broader approach enhances the reliability and generalizability of the findings.

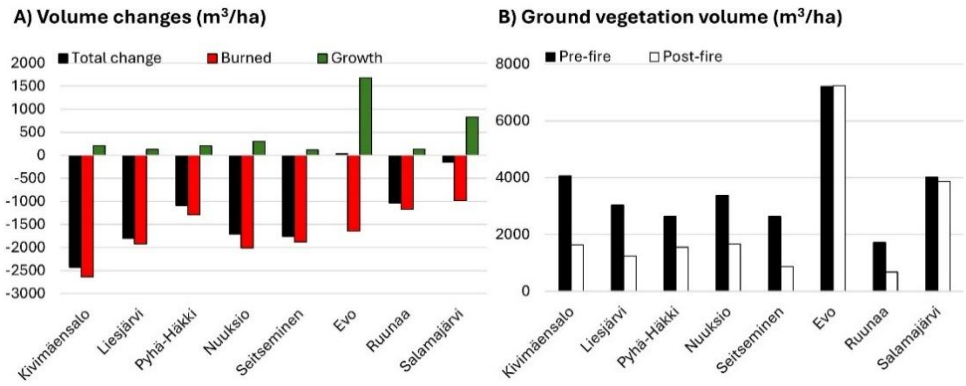

Figure 3. A) Total changes in ground vegetation volume (black) with burned (red) and growth (green) volume. **B)** Ground vegetation volume (including tree stems below 2 m) before and after the controlled burnings (pre- and post-fire, respectively).

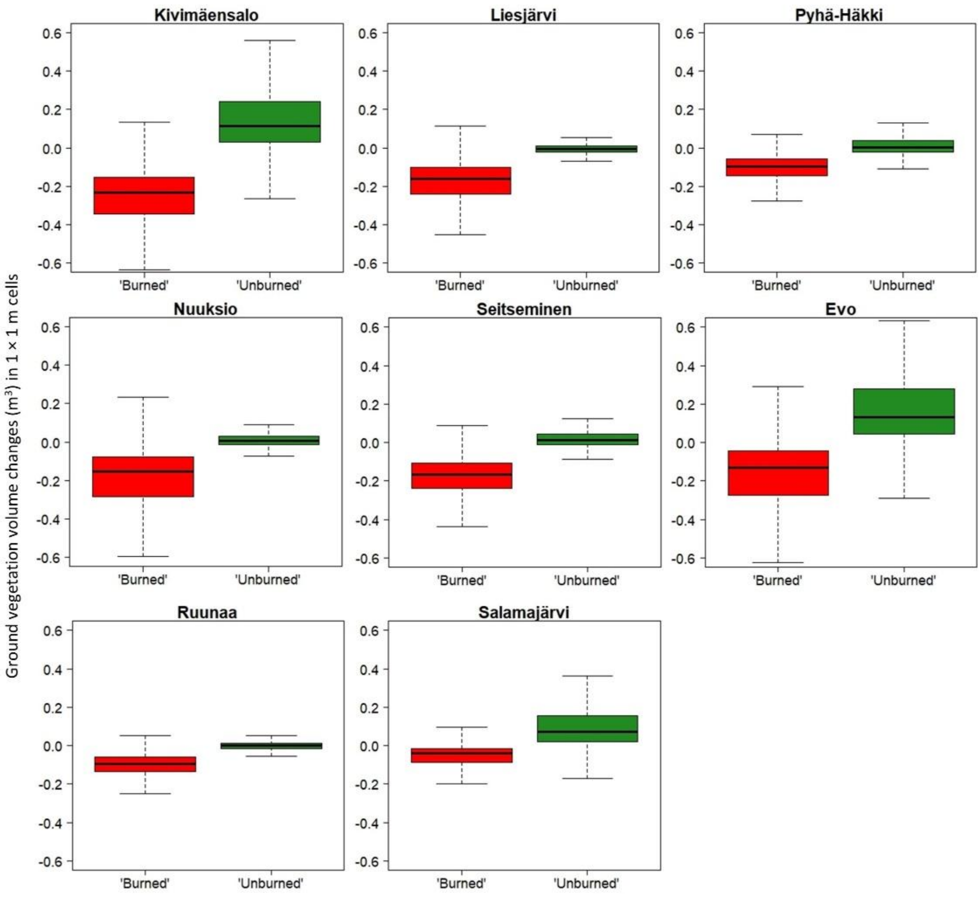

Figure 4. Variation in ground vegetation volume changes (m^3) in 1 × 1 m cells classified as 'burned' (red) and 'unburned' (green) across the test sites. Outliers (0.35% of observations above and below the whiskers) are omitted to enhance data clarity.

3.3 Ground vegetation affects DTMs

Study **II** evaluated the effects of ground vegetation on DTM estimation within the context of point cloud-based forest characterization. The research involved removing ground vegetation through controlled burnings conducted at four boreal forest test sites, and characterizing topography and ground vegetation height before and after the burnings using TLS. It was assumed that post-fire DTMs would more accurately represent the ground surface, showing lower elevation values than pre-fire DTMs due to the removal of occluding vegetation. The study confirmed this, with ground elevation found to be approximately 10 cm lower after vegetation removal.

In burned cells, where ground vegetation was removed, pre-fire DTMs indicated ground surface levels that were, on average, 8–13 cm higher than the corresponding post-fire DTMs, depending on the test site (**Table 6**). These mean differences were statistically significant ($p < 0.001$) in all test sites. Analysis of ΔDTM values between burned and control cells confirmed that these discrepancies resulted from vegetation removal, not geolocation errors between the datasets, as the burned areas featured an average of 9 cm larger |ΔDTM| and 8 cm larger RMSD in the DTM values compared to the control areas (**Table 6**). At the Nuuksio site, control cells showed a positive mean ΔDTM, suggesting post-fire DTMs were higher than pre-fire, likely due to vegetation regrowth between measurements. This anomaly did not affect the results, as the focus was on the burned cells. The variation in ΔDTM within test sites, illustrated by the Nuuksio test site in **Figure 5**, was primarily driven by differences in vegetation height.

Analysis of ΔDTM across the three vegetation height classes revealed that the amount of ground vegetation influenced the degree of DTM overestimation. The lowest vegetation class had an average ΔDTM of –6 cm (±4 cm), the second class had an average of –8 cm (±6 cm), and the third class, with the tallest vegetation, showed an average ΔDTM of –12 cm (±11 cm) (**Figure 6**). Statistical tests confirmed that ΔDTM differed significantly ($p < 0.05$) across all vegetation classes.

Table 6. Mean change in DTM (ΔDTM; pre-fire DTMs subtracted from post-fire DTMs) and root mean square difference (RMSD) between pre- and post-fire DTMs in burned and control areas.

	ΔDTM (cm)		**RMSD (cm)**	
Site	burned	control	burned	control
Nuuksio	–9±11	2±4	15	4
Seitseminen	–11±7	–3±5	13	6
Ruunaa	–8±5	–5±3	9	5
Salamajärvi	–13±8	–2±5	15	5
Average	**–10±8**	**–1±5**	**13**	**5**

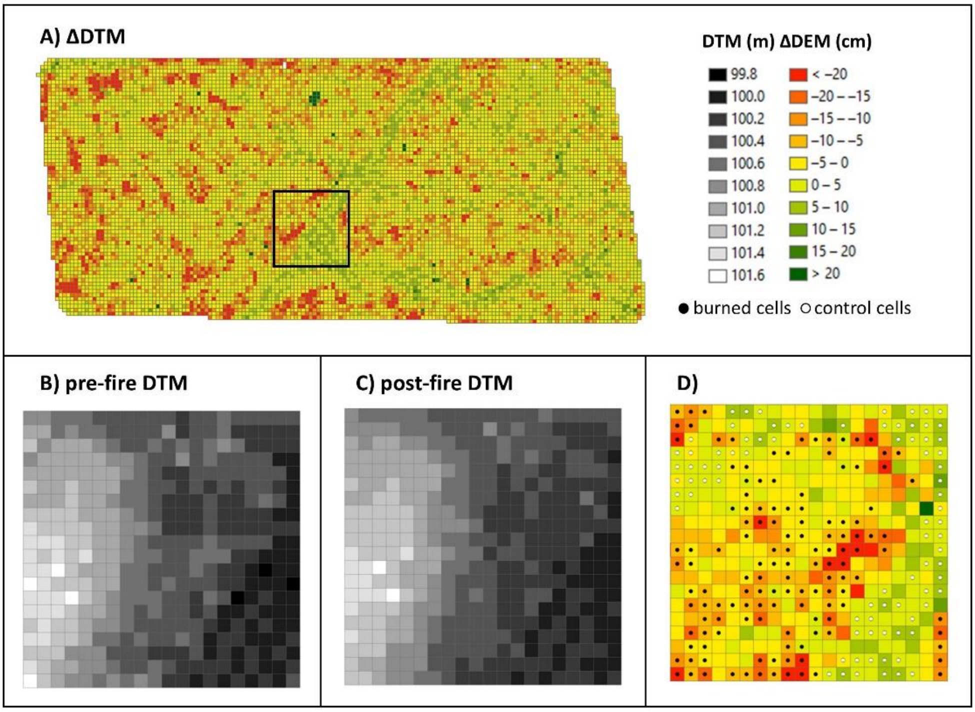

Figure 5. A) Changes in the digital elevation models (ΔDTM; pre-fire DTMs subtracted from post-fire DTMs) of the test site Nuuksio. B) a 20 x 20 m section of pre-fire DTM, C) post-fire DTM, and D) ΔDTM with points marking burned cells (black) and control cells (white) (bottom row).

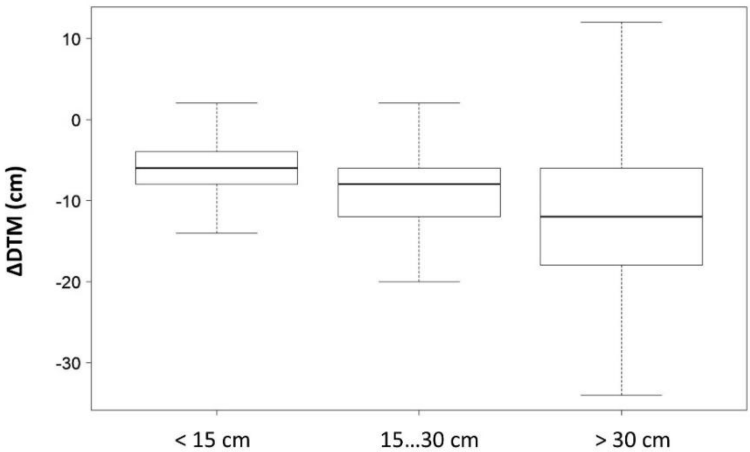

Figure 6. Changes in digital elevation models (ΔDTM; pre-fire DTMs subtracted from post-fire DTMs) within three classes representing different ground vegetation types based on their mean height above the ground within the investigated 1 m x 1 m cells. Negative values indicate overestimation of ground height due to vegetation (i.e., pre-fire DTM appearing higher than post-fire DTM). Bold lines represent the medians, boxes show the interquartile range (IQR), and whiskers extend to 1.5 x IQR, covering the range within a 99.3% confidence interval for normally distributed data. Outliers beyond this range are omitted for clarity.

In the context of forest characterization, the observed DTM overestimation likely leads to an underestimation of tree height and inaccurate stem diameter measurements due to the offset in measurement heights. This, in turn, can cause stem volume to be underestimated. The average ΔDTM of –10 cm resulted in DBH being measured at 1.4 m instead of the actual 1.3 m measurement height. According to the experiments, this offset caused a mean underestimation of DBH by 1.3 mm (0.6%), with the 99% confidence interval ranging from a 0.1 mm overestimation to a 3.7 mm underestimation (**Figure 7**). In the highest vegetation class, the ΔDTM range extended to approximately –30 cm (**Figure 6**), reflecting the most extreme overestimation. This resulted in a 3.6 mm (1.5%) mean underestimation of DBH, with a 99% confidence interval ranging from a 0.4 mm overestimation to a 10.3 mm underestimation.

Inaccurate DTM estimation not only affects DBH measurements but also impacts stem volume calculations. An average ΔDTM of –10 cm led to the omission of the lowest 10 cm of the stem when estimating total volume using pre-fire point clouds. Analysis of 400 trees revealed an average underestimation of stem volume by 4.8 dm^3 (±3.6 dm^3), or 3.1%. In the extreme case of a 30 cm height offset, the underestimation increased to an average of 13.7 dm^3 (±10.3 dm^3), or 8.8%. At the stand level, a 10 cm DTM overestimate caused underestimations in total stem volume, ranging from 2.7 m^3/ha at Nuuksio to 3.6 m^3/ha at Ruunaa, with an overall average of approximately 3 m^3/ha (1.3%). While the impact of DTM inaccuracies may seem minor at a single time point, it can become more significant when tracking structural changes over time. However, if follow-up measurements are taken under similar seasonal conditions, the DTM-induced uncertainty in tree measurements is expected to be minimal.

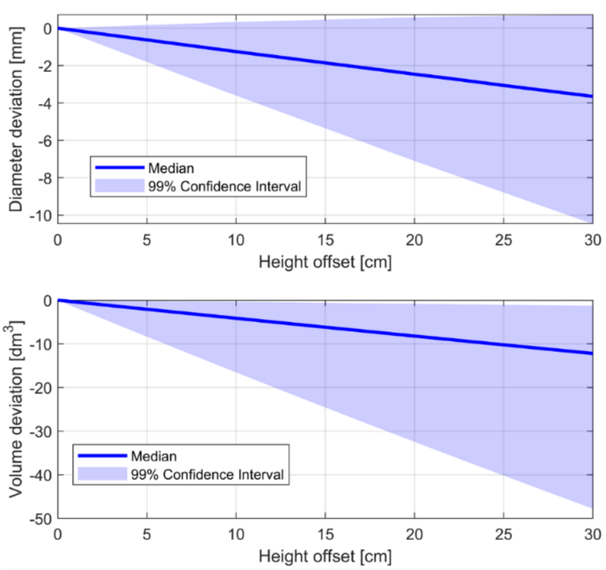

Figure 7. Illustration of the magnitude of stem diameter deviation (top) and volume (bottom) from their actual measured values when the measurement height offsets by 0 to 30 cm higher on the stem due to ground height overestimated because of the presence of ground vegetation. The bold line shows the median deviation, and the shading shows its 99% confidence interval among 400 randomly selected trees (100 trees across each four test sites).

Previous studies have consistently shown that TLS-derived DTMs tend to overestimate elevation by a few centimetres, with discrepancies of up to approximately ten centimetres when compared to values obtained from total station or DGPS measurements at a resolution of 0.3–1.2 m (Guarnieri et al. 2009, Baltensweiler et al. 2017, Jurjević et al., 2021). The results of this study align with these findings, demonstrating that the presence of ground vegetation contributed to an increase in observed elevation values by 8–13 cm. However, it is important to note that this study did not validate TLS-derived DTMs against independent ground elevation measurements. Rather, the study focused on assessing the influence of ground vegetation on DTM accuracy. By comparing DTMs generated from TLS campaigns conducted before and after vegetation removal, the study evaluated how the removal of ground-occluding vegetation affected elevation estimates. Controlled burnings were employed to remove the vegetation. This experimental setup enabled a direct assessment of the effects of vegetation on DTM estimation, which was the primary objective of this study.

The differences observed between pre- and post-fire DTMs can be attributed to the ground vegetation characteristics of the study sites. Around 60% of the 1 m x 1 m cells had a mean vegetation height of <30 cm, with ground-occluding vegetation primarily composed of feather mosses (*Pleurozium schreberi*, *Hylocomium splendens*) and dwarf shrubs (*Vaccinium myrtillus*, *Vaccinium vitis-idaea*) (Palviainen et al. 2005). The degree of DTM overestimation due to ground vegetation may vary across different forest and vegetation types, underscoring the need for further research in diverse ecosystems. For accurate ground characterization in these experiments, a scanner capable of recording multiple returns per laser pulse was used, following the approach suggested by Fun et al. (2014), with the last or only returns employed to ensure accurate capture of the ground surface through occluding vegetation.

The observed systematic overestimation in ground elevation may also be influenced by the TLS measurement geometry. The scanner, mounted 1.7 m above the ground, transmits and receives signals at a low oblique angle, which can result in a longer optical path through vegetation compared to airborne sensors like ALS (Coveney & Fotheringham 2011, Fan et al. 2014). As the distance from the TLS scanner increases, laser returns thought to represent the ground may actually come from vegetation. With a 10 x 10 m scan grid, the theoretical maximum horizontal distance for ground surface observations was about 7.1 m, with an off-nadir angle of 76.5°. A denser grid (e.g., 5 × 5 m) would reduce the obliquity (3.5 m distance, 64.3° angle) but would require more time for measurements. ALS's vertical geometry could provide more accurate ground surface data, though at a lower resolution. ALS offers consistent vertical accuracy across the entire area, whereas TLS-derived DTM uncertainties would vary locally as a function of the scan locations. Future research could compare DTMs derived from various remote sensing techniques, including mobile laser scanning methods such as handheld and drone-based scanners.

3.4 Satellite data detects surface fires

Forest fires are extensively monitored with multispectral satellite time series, as fires alter forest reflectance, leading to lower NBR values. The aim of study **III** was to investigate whether low-intensity surface fires could also be detected using these data. A noticeable decline in NBR values was observed after the surface fires in four out of seven test sites: Kivimäensalo, Liesjärvi, Nuuksio, and Seitseminen (**Figure 6**). These findings suggest that Sentinel-2 within-year time series data can effectively identify low-intensity surface fires. In these four test sites, the NBR-based fire timing estimation closely matched the actual burning time, with an average difference of 2.5 days. In Pyhä-Häkki and Evo, the NBR values also declined after the fires, but the change was less pronounced. In these sites, the average difference between the actual burning time and NBR-based estimation was 23 days. In Salamajärvi, the surface fire was not detected in the recorded dataset.

The variations in the results can be attributed to site-specific factors, including 1) the extent of change in ground vegetation volume, 2) variations in canopy cover, and 3) the number of available NBR observations for each test site. In the test sites where the decline in the NBR values was most pronounced (i.e., Kivimäensalo, Liesjärvi, Nuuksio, and Seitseminen), the TLS-measured total decrease in the ground vegetation volume ranged from 1600 to 2400 m^3/ha (**Table 7**). In contrast, other sites exhibited smaller volume decreases (Pyhä-Häkki and Salamajärvi) or even an increase (Evo). Essentially, in the test sites with more extensive burning, as indicated by the TLS measurements, the occurrence of fire was more discernible in the satellite imagery. The test sites with notable changes in the NBR values also had a lower mean canopy cover (53%) compared to other test sites (72%) (**Table 7**), suggesting that denser canopy cover hindered the fire detection. Additionally, the average number of the post-fire NBR values (i.e., cloud-free observations) was higher (n = 9) in the test sites with notable declines compared to those with smaller changes (n = 3) (**Table 7**). This indicates that a scarcity of cloud-free observations may amplify potential errors in the satellite data, contributing to smaller declines in the NBR values. However, the Kivimäensalo test site was an exception, as there were only two cloud-free observations after the fire, yet a clear change in the NBR values was observed.

In summary, while surface fires generally caused declines in NBR values, these changes were unidentifiable when the forest floor did not burn adequately, when the canopy was too dense, or when there were insufficient cloud-free satellite observations. However, the number of cloud-free observations did not appear to influence the results as significantly as the extent of burned ground vegetation and canopy cover.

Reviewing the NBR values over the five-year period preceding the fire year revealed that, in undisturbed conditions, the NBR values remained relatively stable throughout the summer months (**Figure 6**). This stability suggests that the decline in the NBR values during the fire year was primarily due to surface fires, rather than normal seasonal variation. The slight increase in the NBR values likely reflected the growth of green vegetation. During the fire year, the NBR values started at lower levels compared to previous years, likely due to thinning operations carried out during the previous winter (**Table 2**). However, in Salamajärvi, where no thinnings were conducted, a notable gap between the fire year and previous years was still observed. This discrepancy would need further investigation to be understood.

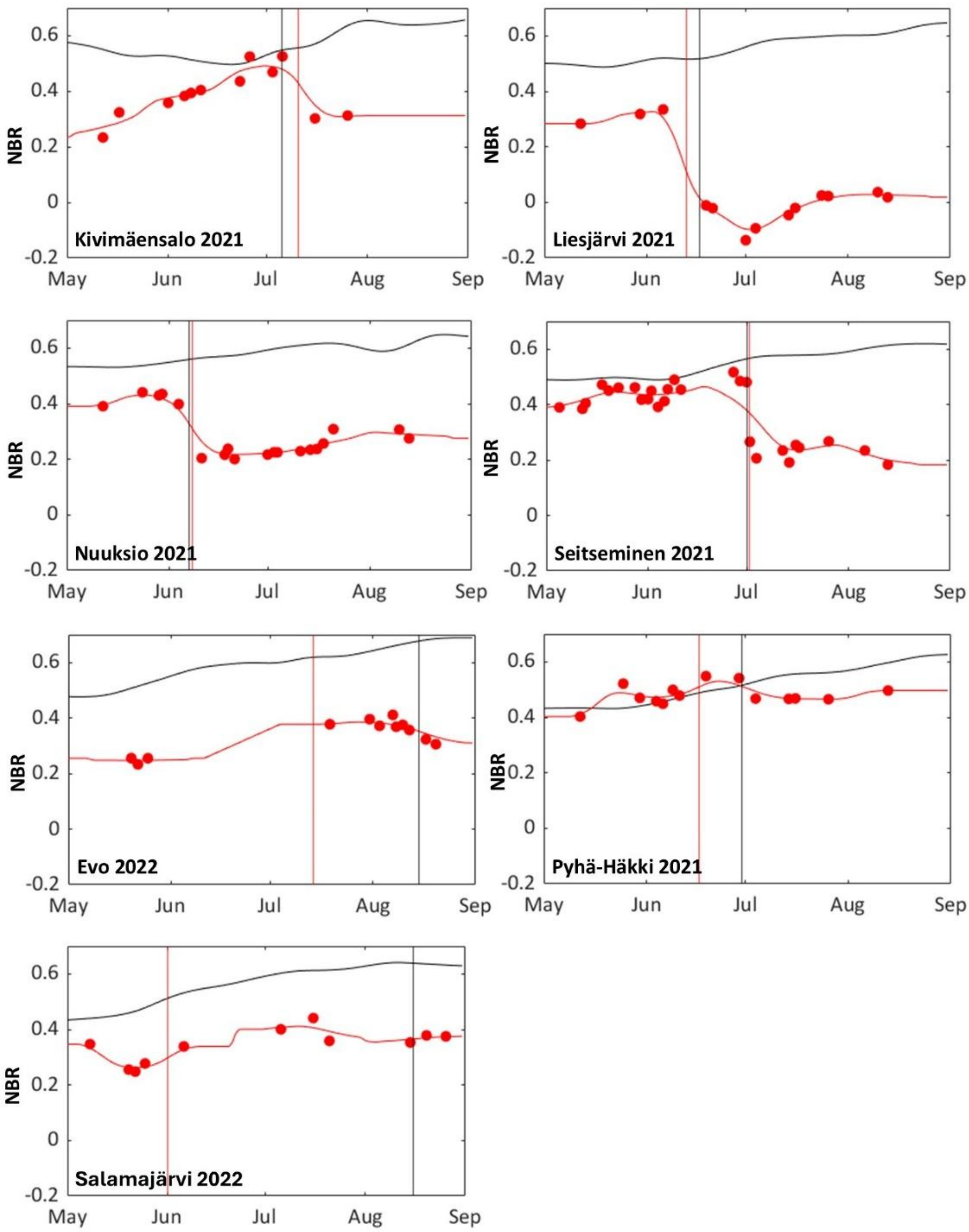

Figure 6. Smoothed development of satellite-based normalized burn ratio (NBR) values during the summer months of the fire year (red curve) and actual values (red dots), trend-removed mean of NBR values for the five years preceding the fire (black curve), actual time of the controlled burning (black vertical line), and an NBR-based signal change point (red vertical line) for each test site.

Table 7. Total changes in ground vegetation volume (vol change) measured using bitemporal terrestrial laser scanning (TLS). Total canopy cover measured using TLS. Number of satellite-based normalized burn ratio (NBR) values (i.e., the number of cloud-free observations) for the fire year. Averages (x̄) for detected and undetected fires.

	Site	**Vol change** (m^3/ha)	**x̄**	**Canopy cover** (%)	**x̄**	**Number of NBR observations** pre-fire	x̄	post-fire	**x̄**
detected	Kivimäensalo	–2400	–1900	59	53	10	9	2	9
	Liesjärvi	–1800		46		3		10	
	Nuuksio	–1600		55		5		14	
	Seitseminen	–1700		53		18		9	
undetect	Evo	300	–300	66	72	10	9	2	3
	Pyhä-Häkki	–1100		75		9		5	
	Salamajärvi	–100		76		9		2	

3.5 Moderate correlation between Sentinel-2 and TLS data

Study **III** also examined the relationship between the satellite-derived dNBR values and TLS-derived volumetric changes in ground vegetation. A moderate negative correlation of –0.5 was observed between the satellite and TLS measurements. As the dNBR values increased and the ground vegetation volumes decreased with greater burn severity, the observed negative correlation aligned with expectations. The R^2 was 0.25, suggesting that 25% of the variance in the dNBR values could be explained by the fire-induced changes on the forest floor. However, this association varied among the test sites, with site-specific R^2 values ranging from 0 to 17% (**Figure 7**). Additionally, observations were visually clustered by the test site, indicating that site-specific conditions influenced the relationship between the satellite and TLS measurements.

To identify factors influencing this relationship, mean dNBR values were analysed across the groups based on volume change and canopy cover. Within the same volume change group, the dNBR values decreased as the canopy cover increased (**Figure 8**). The lowest mean dNBR values were found in unburned areas with high canopy cover, while the highest values occurred in heavily burned areas with low canopy cover. This indicates that dense canopy cover reduces the effectiveness of satellite imagery in detecting changes in forest reflectance caused by small-scale alterations on the forest floor. Similarly, Yin et al. (2020) found that integrating canopy cover into dNBR parameterization significantly improved burn severity estimation.

Given the considerable variability in the relationship between dNBR values and volumetric changes in ground vegetation across the test sites, the effects of canopy cover and site conditions were further investigated through statistical analysis. Initially, changes in ground vegetation volume alone explained 25% of the variation in dNBR values. When canopy cover was included as a second predictor, the R^2 increased to 50%. Adding site information as a random effect further enhanced the model's explanatory power, increasing the R^2 to 84%. Based on the AIC, as well, this mixed-effects model was identified as the most suitable. All predictors in the models were statistically significant (p-values < 0.001).

Kato et al. (2019) utilized TLS to quantify and compare forest structural attributes with Landsat 8 satellite imagery in Canadian boreal forests. They observed a notable, although not statistically significant, relationship between dNBR values and TLS-derived voxels, particularly in the height strata of 0–0.5 m (R^2=56%). Furthermore, the findings of this study align with those of Kato et al. (2019), who indicated that the correlation between voxel counting, and spectral indices reflected ecological responses to site conditions.

This study successfully distinguished the effects of the extent of burned ground vegetation and canopy cover on satellite-based burn severity estimates, though further research is needed, particularly regarding site-specific factors. The variability in the relationship between dNBR values and structural changes in ground vegetation across the test sites appears largely attributable to substantial site-specific differences, such as vegetation types, fuel load, topography, soil moisture, weather conditions, and controlled burning practices. These factors collectively shape fire behaviour and influence post-fire reflectance, emphasizing the importance of accounting for local conditions when interpreting remote sensing data related to forest fire dynamics.

Detecting surface fires from satellites is more challenging than identifying crown fires, primarily due to the limited capability of optical satellites to penetrate the tree canopy. Therefore, understanding the effectiveness of surface fire detection is crucial, and this study offers valuable insights into this issue. Specifically, study **III** explored how multispectral satellite imagery can be employed to observe fire-induced changes in boreal forests, emphasizing the factors influencing the relationship between forest reflectance and ground vegetation changes. By integrating on-site laser scanning with satellite-based burn severity estimates, the study successfully demonstrated the ability to identify low-intensity surface fires and deepen our understanding of fire effects across different forest layers, thereby advancing research in fire ecology.

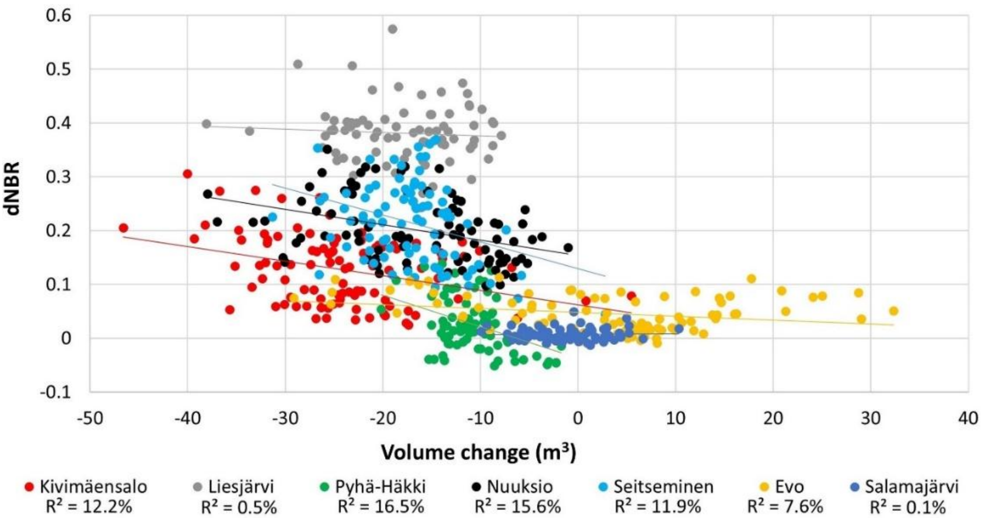

Figure 7. Scatterplot of satellite-based difference normalized burn ratio (dNBR) in relation to volumetric changes in ground vegetation (m^3) measured using terrestrial laser scanning (TLS) within 10 × 10 m cells. R^2=coefficient of determination.

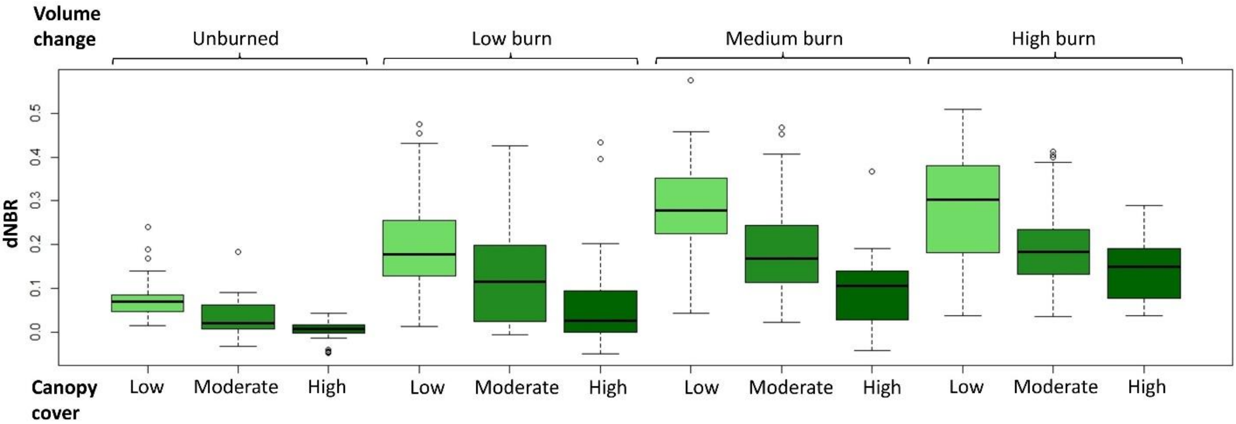

Figure 8. Boxplots of satellite-based difference normalized burn ratio (dNBR) in ground vegetation volume change groups (unburned, low burn, medium burn, high burn) and canopy cover groups (low, moderate, high) measured by terrestrial laser scanning (TLS).

3.6 Challenges and future directions

Surface differencing, the method used in all sub-studies to quantify volumetric changes in ground vegetation, assumes that the space beneath the observed vegetation surface is fully occupied by vegetation or fuel load. This assumption may lead to an overestimation of volume in cells where the highest point is represented by loose branches or small twigs, for example. Alternative methods for estimating ground vegetation volume include the convex hull method and voxel counting (Loudermilk et al. 2009, Olsoy et al. 2014, Graeves et al. 2015). Surface differencing was chosen for this thesis because, for instance, Zhao et al. (2021) demonstrated that it has the strongest correlation with field-measured biomass when estimating shrub volume in grasslands, outperforming other methods. While comparing results obtained from different methods using boreal forest data could provide valuable insights, the primary focus should be on carefully validating the selected method, as done in study **I**.

In studies **I** and **II**, 1 × 1 m cells were categorized based on the proportion of 0.1 × 0.1 m cells they contained. In study **I**, a cell was classified as ‘burned’ if more than half of the associated 0.1 × 0.1 m cells showed a negative change in vegetation height. The approach aimed to base the classification on recognizing a sufficient proportion of a 1 × 1 m cell area representing decreased change, while the magnitude of change was not the determinant. This was intended to avoid decisions based on single – possibly erroneous – observations, enhancing the robustness of the developed method. In contrast, study **II** identified burned cells by a decrease in ground vegetation height of more than 5 cm in at least 80% of its area. This minimum decrease threshold was chosen to ensure that the identified cells represented surface patches where the bare ground was exposed to the laser scanner for enhanced DTM reconstruction. It also aimed at considering the alignment accuracy of 3.2 cm in the Z-direction for the pre- and post-fire point clouds. However, alternative thresholds in the studies might have yielded slightly different numerical results, though the overall findings are expected to remain consistent. For instance, in study **II**, a higher height threshold might have led to even more pronounced differences between pre- and post-fire DTMs. It should be noted that some of the applied parameters may be sensitive to the applied technology, the level of detail of the attained point clouds as well as the forest conditions where the methodology was developed and tested. Future research is therefore required for assessing the feasibility of applying the methodology outside the experimental conditions used here.

The pre-fire TLS measurements were conducted an average of 20 days before the controlled burnings, and post-fire measurements 40 days afterward. As a result, unburned areas had an average of 70 days to continue growing (**Table 2**). Although all test sites were used only in study **I**, this timing issue might contribute to the findings obtained in all sub-studies. If vegetation growth occurred between pre-fire measurements and burning, the magnitude of burned vegetation may have been underestimated, while the increased volume may have been overestimated. The vegetation in burned areas likely remained stable until post-fire measurements. To improve accuracy of the point cloud-based assessments of the magnitude of burned vegetation, future TLS campaigns should be scheduled closer to the burning dates. However, this can be challenging due to the dependency of controlled burnings on weather conditions and, as in this case, if the burnings are conducted by an external party. Acquiring the point cloud data using a more agile laser scanning technology utilizing a moving platform may provide a solution. However, future research is needed to assess the feasibility of such approaches in assessing the magnitude of burned vegetation.

The TLS-based estimates of the volumetric extent of ground vegetation exposed to fire can serve as a basis for related biomass estimation, but this relationship is significantly influenced by the density, distribution, and characteristics of the vegetation occupying the observed volume. Accurate biomass estimation would necessitate destructive sampling, which involves collecting, drying, and weighing vegetation samples (Houghton 2008). The biomass estimates could then be converted into CO_2 equivalents, facilitating assessments of the climatic impacts of low-intensity fires and enabling a more precise understanding of carbon fluxes. Additionally, the vegetation changes can be viewed in terms of fuel consumption, as the vegetation consumed represents fuel burned, which is an important factor for estimating fire emissions and effects. The use of multispectral laser scanning would enable incorporating both geometric and spectral properties of the investigated volumetric units (voxels), which would aid in differentiating various material categories that are destructively sampled for accurate biomass estimation. Additionally, by monitoring post-fire vegetation recovery and tree mortality, future research could evaluate the longer-term ecological effects of surface fires, thereby contributing to a more comprehensive understanding of forest dynamics and resilience.

4 CONCLUSIONS

This thesis quantified changes in ground vegetation resulting from low-intensity surface fires in Scots pine-dominated boreal forests using TLS point clouds. Bitemporal TLS campaigns were conducted at eight one-hectare test sites in Finland, where controlled burnings simulating surface fires were performed between the measurements.

A classification method based on changes in vegetation height was developed to identify burned areas with experiments demonstrating that TLS is sensitive enough to capture fine-scale changes on the forest floor. This method benefits practitioners who conduct controlled burnings and assess their effectiveness. Additionally, bitemporal TLS proved effective for estimating fire-induced volumetric changes in ground vegetation. The considerable variability observed both between and within controlled burning sites highlights the complex dynamics of surface fires and emphasizes the need for studies across diverse environmental conditions and sufficiently large experimental plots.

The experimental setup of this thesis enabled an examination of how ground vegetation influences the accuracy of TLS-based estimates of bare ground elevation. Pre- and post-fire DTMs were generated and compared for burned areas, revealing an average decrease of 10 cm following the removal of ground vegetation. Comparing burned and unburned control areas confirmed that the observed DTM changes were primarily due to vegetation removal. Additionally, taller ground vegetation resulted in greater uncertainty in DTM. Inaccurate DTMs can distort key forest attributes, with this study revealing that individual tree stem volume was underestimated by 3.1% and stand-level stem volume by 1.3%. This experiment offered valuable insights into quantifying vegetation-induced uncertainty in DTMs, improving TLS applications in densely vegetated forests, and emphasizing the need to address such uncertainty in topographic characterization.

The TLS-derived observations from surface fires were compared with burn severity estimates based on multispectral satellite imagery. The Sentinel-2 time series effectively identified most surface fires, showing a significant decrease in NBR values, which reflect fire impact on the forest ecosystem. However, identifying surface fires in areas with denser canopy cover and less burned ground vegetation proved more challenging for satellite data. A moderate negative correlation was observed between spectral and volumetric changes, indicating that higher satellite-based burn severity estimates aligned with a greater decrease in ground vegetation volume measured by TLS. Further analysis confirmed that both canopy cover and, in particular, site-specific conditions significantly influenced the correlation between spectral and volumetric changes.

In conclusion, this thesis demonstrated the effectiveness of TLS in capturing fine-scale, fire-induced changes in ground vegetation, providing valuable insights into the complexities of surface fires. The findings underscore the potential for integrating TLS data with satellite-based burn severity estimates to improve the accuracy of forest fire monitoring and to better understand the factors influencing burn severity within fire-affected areas. By refining assessment methods across different forest layers, this research supports improved fire management strategies and advances understanding of the ecological effects of surface fires in boreal ecosystems.

REFERENCES

Abegg M, Kükenbrink D, Zell J, Schaepman ME, Morsdorf F (2017) Terrestrial laser scanning for forest inventories – tree diameter distribution and scanner location impact on occlusion. Forests 8, article id 184. https://doi.org/10.3390/f8060184

Amitrano D, Di Martino G, Guida R, Iervolino P, Iodice A, Papa MN, Riccio D, Ruello G (2021) Earth environmental monitoring using multi-temporal synthetic aperture radar: A critical review of selected applications. Remote Sens 13, article id 604. https://doi.org/10.3390/rs13040604

Avetisyan D, Velizarova E, Filchev L (2023) Post-fire forest vegetation state monitoring through satellite remote sensing and in situ data. Remote Sens 14, article id 6266. https://doi.org/10.3390/rs14246266

Baltensweiler A, Walthert L, Ginzler C, Sutter F, Purves RS, Hanewinkel M (2017) Terrestrial laser scanning improves digital elevation models and topsoil pH modelling in regions with complex topography and dense vegetation. Environ Model Softw 95: 13–21. https://doi.org/10.1016/j.envsoft.2017.05.009

Bell AJ (2023) Like moths to a flame: A review of what we know about pyrophilic insects. For Ecol Manage 528, article id 120629. https://doi.org/10.1016/j.foreco.2022.120629

Bohlin J, Wallerman J, Fransson JES (2012) Forest variable estimation using photogrammetric matching of digital aerial images in combination with a high-resolution DEM. Scan J For Res 27: 692–699. https://doi.org/10.1080/02827581.2012.686625

Buriánek V, Novotný R, Hellebrandová K, Šrámek V (2013) Ground vegetation as an important factor in the biodiversity of forest ecosystems and its evaluation in regard to nitrogen deposition. J. For. Sci. 59: 238–252. https://doi.org/10.17221/16/2013-JFS

Bürgmann R, Rosen PA, Fielding EJ (2000) Synthetic aperture radar interferometry to measure Earth’s surface topography and its deformation. Annu Rev Earth Planet Sci 28: 169–209. https://doi.org/10.1146/annurev.earth.28.1.169.

Cai L, Wang M (2022) Is the RdNBR a better estimator of wildfire burn severity than the dNBR? A discussion and case study in southeast China. Geocarto Int 37: 758–772. https://doi.org/10.1080/10106049.2020.1737973

Cajander AK (1926) The theory of forest types. Acta For Fen 29(3), article id 7193. https://doi.org/10.14214/aff.7193

Calders K, Adams J, Armston J, Bartholomeus H, Bauwens S, Patrick Bentley L, Chave J, Danson FM, Demol M, Disney M, Gaulton R, Krishna Moorthy SM, Levick SR, Saarinen N, Schaaf C, Stovall A, Terryn L, Wilkes P, Verbeeck H (2020) Terrestrial laser scanning in forest ecology: Expanding the horizon. Remote Sens Environ 251, article id 112102. https://doi.org/10.1016/j.rse.2020.112102

Cameron HA, Schroeder D, Beverly JL (2022) Predicting black spruce fuel characteristics with Airborne Laser Scanning (ALS). Int J Wildland Fire 31: 124–135. https://doi.org/10.1071/WF21004

Cardil A, Monedero S, Schag G, de-Miguel S, Tapia M, Stoof CR, Silva CA, Mohan M, Cardil A, Ramirez J (2021) Fire behavior modeling for operational decision-making. Curr Opin Environ Sci Health 23, article id 100291. https://doi.org/10.1016/j.coesh.2021.100291

Corona P, Lamonaca A, Chirici G (2008) Remote sensing support for post fire forest management. iForest 1: 6–12. https://doi.org/10.3832/ifor0305-0010006

Corradino C, Malaguti AB, Ramsey MS, Del Negro C (2024) Quantitative assessment of volcanic thermal activity from space using an Isolation Forest machine learning algorithm. Remote Sens 16, article id 2001. https://doi.org/10.3390/rs16112001

Coveney S, Fotheringham AS (2011) Terrestrial laser scan error in the presence of dense ground vegetation. Photogramm Rec 26: 307–324. https://doi.org/10.1111/j.1477-9730.2011.00647.x

Dassot M, Constant T, Fournier M (2011) The use of terrestrial LiDAR technology in forest science: application fields, benefits and challenges. Ann For Sci 68: 959–974. https://doi.org/10.1007/s13595-011-0102-2

Douglas ES, Martel J, Zhan L, Howe G, Hewawasam K, Marshall RS, Schaaf CL, Cook TA, Newnham GJ, Strahler A, Chakrabarti S (2015) Finding leaves in the forest: The dual-wavelength Echidna lidar. IEEE Geosci Remote Sens Lett 12: 776–780. https://doi.org/10.1109/LGRS.2014.2361812

Epting J, Verbyla D (2005) Landscape-level interactions of prefire vegetation, burn severity, and postfire vegetation over a 16-year period in interior Alaska. Can J For Res 35: 1367–1377. https://doi.org/10.1139/x05-060

Escuin S, Navarro R, Fernández P (2008) Fire severity assessment by using NBR (Normalized Burn Ratio) and NDVI (Normalized Difference Vegetation Index) derived from LANDSAT TM/ETM images. Int J Remote Sens 29: 1053–1073. https://doi.org/10.1080/01431160701281072

Fan L, Powrie W, Smethurst J, Atkinson PM, Einstein H (2014) The effect of short ground vegetation on terrestrial laser scans at a local scale. ISPRS J Photogramm Remote Sens 95: 42–52. https://doi.org/10.1016/j.isprsjprs.2014.06.003

Fan L, Atkinson PM (2015) Accuracy of digital elevation models derived from terrestrial laser scanning data. IEEE Geosci Remote Sens Lett 12: 1923–1927. https://doi.org/10.1109/LGRS.2015.2438394

FAO (2020) Global forest resources assessment 2020. Main report. Food and Agriculture Organization of the United Nations, Rome. https://doi.org/10.4060/ca9825en

FAO (2024) The state of the world's forests 2024 – Forest-sector innovations towards a more sustainable future. Food and Agriculture Organization of the United Nations, Rome. https://doi.org/10.4060/cd1211en

Fassnacht FE, Schmidt-Riese E, Kattenborn T, Hernández J (2021) Explaining Sentinel 2-based dNBR and RdNBR variability with reference data from the bird's eye (UAS) perspective. Int J App Earth Obs Geoinf 95, article id 102262. https://doi.org/10.1016/j.jag.2020.102262

Fernández-García V, Calvo L, Suárez-Seoane S, Macros E (2023a) Remote sensing advances in fire science: From fire predictors to post-fire monitoring. Remote Sens 15, article id 4930. https://doi.org/10.3390/rs15204930

Fernández-García V, Alonso-González E (2023b) Global patterns and dynamics of burned area and burn severity. Remote Sens 15, article id 3401. https://doi.org/10.3390/rs15133401

Flannigan MD, Amiro BD, Logan KA, Stocks BJ, Wotton BM (2005) Forest fires and climate change in the 21st century. Mitig Adapt Strateg Glob Chang 11: 847–859. https://doi.org/10.1007/s11027-005-9020-7

Fouladinejad F, Matkan A, Hajeb M, Brakhasi F (2019) History and applications of space-borne lidars. Int Arch Photogramm Remote Sens Spatial Inf Sci XLII-4/W18: 407–414. https://doi.org/10.5194/isprs-archives-XLII-4-W18-407-2019

French NH, Kasischke ES, Hall RJ, Murphy KA, Verbyla DL, Hoy EE, Allen JL (2008) Using Landsat data to assess fire and burn severity in the North American boreal forest

region: An overview and summary of results. Int J Wildland Fire 17: 443–462. https://doi.org/10.1071/wf08007
Friedli M, Kirchgessner N, Grieder C, Liebisch F, Mannale M, Walter A (2016) Terrestrial 3D laser scanning to track the increase in canopy height of both monocot and dicot crop species under field conditions. Plant Methods 12, article id 9. https://doi.org/10.1186/s13007-016-0109-7
Gajendiran K, Kandasamy S, Narayanan M (2024) Influences of wildfire on the forest ecosystem and climate change: A comprehensive study. Environ Res 240, article id 117537. https://doi.org/10.1016/j.envres.2023.117537
Gallagher MR, Skowronski NS, Lathrop RG, McWilliams T, Green EJ (2020) An improved approach for selecting and validating burn severity indices in forested landscapes. Can R Remote Sens 46: 100–111. https://doi.org/10.1080/07038992.2020.1735931
Gallagher MR, Maxwell AE, Guillén LA, Everland A, Loudermilk EL, Skowronski NS (2021) Estimation of plot-level burn severity using terrestrial laser scanning. Remote Sens 13, article id 4168. https://doi.org/10.3390/rs13204168
García-Morote FA, Martínez-García E, Andrés-Abellán M, Caballero ER, Miettinen H, López-Serrano FR (2017) Direct seeding of *Pinus halepensis* Mill. for recovery of burned semi-arid forests: Implications for post-fire management for improving natural regeneration. Forests 8, article id 353. https://doi.org/10.3390/f8090353
Gauthier S, Bernier P, Kuuluvainen T, Shvidenko AZ, Schepaschenko DG (2015) Boreal forest health and global change. Science 349: 819–822. https://doi.org/10.1126/science.aaa9092
Gitas I, Mitri G, Veraverbeke S, Polychronaki A (2012) Advances in remote sensing of post-fire vegetation recovery monitoring – A review. In: Fatoyinbo T (ed) Remote sensing of biomass. Principles and applications. InTechOpen, Rijeka, pp 143–176. http://dx.doi.org/10.5772/696
Goodenough DG, Chen H, Richardson A, Cloude S, Hong W, Li Y (2011) Mapping fire scars using Radarsat-2 polarimetric SAR data. Can J Remote Sens 37: 500–509. https://doi.org/10.5589/m11-060
Greaves HE, Vierling LA, Eitel JUH, Boelman NT, Magney TS, Prager CM, Griffin KL (2015) Estimating aboveground biomass and leaf area of low-stature Arctic shrubs with terrestrial LiDAR. Remote Sens Environ 164: 26–35. https://doi.org/10.1016/j.rse.2015.02.023
Greene DF, Michaletz ST (2015) The role of fire in forest ecosystems. In: Peh KS-H, Corlett RT, Bergeron Y (eds) Routledge handbook of forest ecology. Routledge, London, pp 114–126.
Guarnieri A, Vettore A, Pirotti F, Menenti M, Marani M (2009) Retrieval of small-relief marsh morphology from Terrestrial Laser Scanner, optimal spatial filtering, and laser return intensity. Geomorphology 113: 12–20. https://doi.org/10.1016/j.geomorph.2009.06.005
Gupta V, Reinke KJ, Jones SD, Wallace L, Holden L (2015) Assessing metrics for estimating fire induced change in the forest understorey structure using terrestrial laser scanning. Remote Sens 7: 8180–8201. https://doi.org/10.3390/rs70608180
Hendel I–G, Ross GM (2020) Efficacy of remote sensing in early forest fire detection: A thermal sensor comparison. Can J Remote Sens 46: 414–428. https://doi.org/10.1080/07038992.2020.1776597
Hilker T, van Leeuwen M, Coops NC, Wulder MA, Newnham GJ, Jupp DLB, Culvenor DS (2010) Comparing canopy metrics derived from terrestrial and airborne laser scanning

in a Douglas-fir dominated forest stand. Trees 24: 819–832. https://doi.org/10.1007/s00468-010-0452-7
Hodgson ME, Bresnahan P (2004) Accuracy of airborne lidar-derived elevation: Empirical assessment and error budget. Photogramm Eng Remote Sens 70: 331–339. https://doi.org/10.14358/PERS.70.3.331
Hopkinson C, Chasmer LE, Sass G, Creed IF, Sitar M, Kalbfleisch W, Treitz P (2005) Vegetation class dependent errors in lidar ground elevation and canopy height estimates in a boreal wetland environment. Can J Remote Sens 31: 191–206. https://doi.org/10.5589/m05-007
Hosseini M, Lim S (2023) Burned area detection using Sentinel-1 SAR data: A case study of Kangaroo Island, South Australia. Appl Geogr 151, article id 102854. https://doi.org/10.1016/j.apgeog.2022.102854
Hosseini S, Urbanski SP, Dixit P, Qi L, Burling IR, Yokelson RJ, Johnson TJ, Shrivastava M, Jung HS, Weise DR, Miller JW, Cocker III DR (2013) Laboratory characterization of PM emissions from combustion of wildland biomass fuels. J Geophys Res: Atmos 118: 9914–9929. https://doi.org/10.1002/jgrd.50481
Houghton RA (2008) Biomass. In: Jørgensen SE, Fath BD (eds) Encyclopedia of ecology. Elsevier, Amsterdam, pp 448–453.
Hudak AT, Morgan P, Bobbitt MJ, Smith AMS, Lewis SA, Lentile LB, Robichaud PR, Clark JT, McKinley RA (2007) The relationship of multispectral satellite imagery to immediate fire effects. Fire Ecol 3: 64–90. https://doi.org/10.4996/fireecology.0301064
Isenburg M (2021) LAStools – efficient LiDAR processing software (version 211218, academic). http://rapidlasso.com/LAStools. Accessed 19 October 2023.
Ji L, Zhang L, Wylie BK, Rover J (2011) On the terminology of the spectral vegetation index (NIR − SWIR)/(NIR + SWIR). Int J Remote Sens 32: 6901-6909. https://doi.org/10.1080/01431161.2010.510811
Jonsson BG, Kruys N, Ranius T (2005) Ecology of species living on dead wood – Lessons for dead wood management. Silva Fenn 39: 289–309. https://doi.org/10.14214/sf.390
Jurjević L, Gašparović M, Liang X, Balenović I (2021) Assessment of close-range remote sensing methods for DTM estimation in a lowland deciduous forest. Remote Sens 13, article id 2063. https://doi.org/10.3390/rs13112063
Kaku K (2019) Satellite remote sensing for disaster management support: A holistic and staged approach based on case studies in Sentinel Asia. Int J Disaster Risk Reduct 33: 417–432. https://doi.org/10.1016/j.ijdrr.2018.09.015
Karjalainen J (1994) Tuli pohjoisissa havumetsissä ja metsänhoidollinen kulotus. [Fire in northern coniferous forests and restorative burning]. Metsähallitus, Vantaa.
Kasniza Jumari NAS, Ahmed AN, Huang YF, Ng JL, Koo CH, Chong KL, Sherif M, Elshafie A (2023) Analysis of urban heat islands with landsat satellite images and GIS in Kuala Lumpur Metropolitan City. Heliyon 9, article id e18424. https://doi.org/10.1016/j.heliyon.2023.e18424
Kato A, Moskal LM, Batchelor JL, Thau D, Hudak AT (2019) Relationships between satellite-based spectral burned ratios and terrestrial laser scanning. Forests 10, article id 444. https://doi.org/10.3390/f10050444
Kauranne T, Pyankov S, Junttila V, Kedrov A, Tarasov A, Kuzmin A, Peuhkurinen J, Villikka M, Vartio V-M, Sirparanta S (2017) Airborne laser scanning based forest inventory: Comparison of experimental results for the Perm region, Russia and prior results from Finland. Forests 8, article id 72. https://doi.org/10.3390/f8030072

Keeley JE, Fotheringham CJ (2000) Role of fire in regeneration from seed. In: Fenner M (ed) Seeds. The ecology of regeneration in plant communities. CABI Publishing, Wallingford, pp 311–330.
Kennedy MC, Johnson MC, Fallon K, Mayer D (2019) How big is enough? Vegetation structure impacts effective fuel treatment width and forest resiliency. Ecosphere 10, article id e02573. https://doi.org/10.1002/ecs2.2573
Key CH, Benson NC (2006) Landscape Assessment (LA) sampling and analysis methods. General Technical Report 164. USDA Forest Service, Fort Collins.
Kim S, Lee I, Lee M (2012) Lidar waveform simulation over complex targets. Int Arch Photogramm Remote Sens Spatial Inf Sci XXXIX-B7: 517–522. https://doi.org/10.5194/isprsarchives-XXXIX-B7-517-2012
Kreider MR, Higuera PE, Parks SA, Rice WL, White N, Larson AJ (2024) Fire suppression makes wildfires more severe and accentuates impacts of climate change and fuel accumulation. Nat Commun 15, article id 2412. https://doi.org/10.1038/s41467-024-46702-0
Laurila J, Vierula J (2020) Kulotusopas. [Controlled burning guide]. Suomen metsäkeskus, Seinäjoki.
Lazzeri G, Frodella W, Rossi G, Moretti S (2021) Multitemporal mapping of post-fire land cover using multiplatform PRISMA hyperspectral and Sentinel-UAV multispectral data: Insights from case studies in Portugal and Italy. Sensors 21, article id 3982. https://doi.org/10.3390/s21123982
Leblon B, Bourgeau-Chavez L, San-Miguel-Ayanz J (2012) Use of remote sensing in wildfire management. In: Curkovic S (ed) Sustainable development. Authoritative and leading edge content for environmental management. IntechOpen, Rijeka, pp 55–82. http://dx.doi.org/10.5772/45829
Lemberg K, Puttonen P (2002) Kulottajan käsikirja. [Handbook for controlled burning]. Metsälehti Kustannus, Helsinki.
Lentile LB, Holden ZA, Smith AMS, Falkowski MJ, Hudak AT, Morgan P, Lewis SA, Gessler PE, Benson NC (2006) Remote sensing techniques to assess active fire characteristics and post-fire effects. Int J Wildland Fire 15, article id 319. https://doi.org/10.1071/WF05097
Liang X, Kankare V, Hyyppä J, Wang Y, Kukko A, Haggrén H, Yu X, Kaartinen H, Jaakkola A, Guan F, Holopainen M, Vastaranta M (2016) Terrestrial laser scanning in forest inventories. ISPRS J Photogramm Remote Sens 115: 63–77. http://dx.doi.org/10.1016/j.isprsjprs.2016.01.006
Lin Y, Jaakkola A, Hyyppä J, Kaartinen H (2010) From TLS to VLS: Biomass estimation at individual tree level. Remote Sens 2: 1864–1879. https://doi.org/10.3390/rs2081864
Lindberg H, Heikkilä TV, Vanha-Majamaa I (2011) Suomen metsien paloainekset – kohti parempaa tulen hallintaa [Finnish forest fuels – towards improved fire management]. Metsäntutkimuslaitos, Vantaa.
Lindberg H, Saaristo L, Nieminen A (2018) Tuli takaisin metsiin – kulotuksiin kannustamisen perusteet, tavoitteet ja tukeminen [Returning fire to forests – basics, objectives, and support for controlled burning]. Tapio, Helsinki.
López García MJ, Caselles V (1991) Mapping burns and natural reforestation using thematic Mapper data. Geocarto Int 6: 31–37. https://doi.org/10.1080/10106049109354290
Loudermilk EL, Hiers JK, O'Brien JJ, Mitchell RJ, Singhania A, Fernandez JC, Cropper Jr WP, Slatton KC (2009) Ground-based LIDAR: A novel approach to quantify fine-scale fuelbed characteristics. Int J Wildland Fire 18: 676–685. https://doi.org/10.1071/WF07138

Loudermilk EL, Pokswinski S, Hawley CM, Maxwell A, Gallagher MR, Skowronski NS, Hudak AT, Hoffman C, Hiers JK (2023) Terrestrial laser scan metrics predict surface vegetation biomass and consumption in a frequently burned southeastern U.S. ecosystem. Fire 6, article id 151. https://doi.org/10.3390/fire6040151

Ludwig F, de Kroon H, Berendse F, Prins HHT (2004) The influence of savanna trees on nutrient, water and light availability and the understorey vegetation. Plant Ecol 170: 93–105. https://doi.org/10.1023/B:VEGE.0000019023.29636.92

Magnussen S, Wulder MA (2012) Post-fire canopy height recovery in Canada's boreal forests using airborne laser scanner (ALS). Remote Sens 4: 1600–1616. https://doi.org/10.3390/rs4061600

Malambo L, Popescu SC, Murray SC, Putman E, Pugh NA, Horne DW, Richardson G, Sheridan R, Rooney WL, Avant R, Vidrine M, McCutchen B, Baltensperger D, Bishop M (2018) Multitemporal field-based plant height estimation using 3D point clouds generated from small unmanned aerial systems high-resolution imagery. Int J Appl Earth Obs Geoinf 64: 31–42. https://doi.org/10.1016/j.jag.2017.08.014

Mallinis G, Mitsopoulos I, Chrysafi I (2018) Evaluating and comparing Sentinel 2A and Landsat-8 Operational Land Imager (OLI) spectral indices for estimating fire severity in a Mediterranean pine ecosystem of Greece. GISci Remote Sens 55: 1–18. https://doi.org/10.1080/15481603.2017.1354803

Mandlburger G, Pfennigbauer M, Pfeifer N (2013) Analyzing near water surface penetration in laser bathymetry – A case study at the River Pielach. ISPRS Ann Photogramm Remote Sens Spatial Inf Sci II-5/W2: 175–180. https://doi.org/10.5194/isprsannals-II-5-W2-175-2013

Marozas V, Racinskas J, Bartkevicius E (2007) Dynamics of ground vegetation after surface fires in hemiboreal *Pinus sylvestris* forests. For Ecol Manag 250: 47–55. https://doi.org/10.1016/j.foreco.2007.03.008

McCarley TR, Hudak AT, Bright BC, Cronan J, Eagle P, Ottmar RD, Watts AC (2024) Generating fuel consumption maps on prescribed fire experiments from airborne laser scanning. Int J Wildland Fire 33, article id WF23160. https://doi.org/10.1071/WF23160

Melin M, Shapiro AC, Glover-Kapfer P (2017) LIDAR for ecology and conservation. WWF Conservation Technology Series 1(3), Woking.

Michałowska M, Rapiński J (2021) A review of tree species classification based on airborne LiDAR data and applied classifiers. Remote Sens 13, article id 353. https://doi.org/10.3390/rs13030353

Miller J, Böhnisch A, Ludwig R, Brunner MI (2024) Climate change impacts on regional fire weather in heterogeneous landscapes of central Europe. Nat Hazards Earth Syst Sci 24: 411–428. https://doi.org/10.5194/nhess-24-411-2024

Miller JD, Thode AE (2007) Quantifying burn severity in a heterogeneous landscape with a relative version of the delta Normalized Burn Ratio (dNBR). Remote Sens Environ 109: 66–80. https://doi.org/10.1016/j.rse.2006.12.006

Montealegre AL, Lamelas MT, Tanase MA, de la Riva J (2014) Forest fire severity assessment using ALS data in a Mediterranean environment. Remote Sens 6: 4240–4265. https://doi.org/10.3390/rs6054240

Montealegre AL, Lamelas MT, de la Riva J (2015) Interpolation routines assessment in ALS-derived digital elevation models for forestry applications. Remote Sens 7: 8631–8654. https://doi.org/10.3390/rs70708631

Moskal LM, Zheng G (2012) Retrieving forest inventory variables with terrestrial laser scanning (TLS) in urban heterogeneous forest. Remote Sens 4: 1–20. https://doi.org/10.3390/rs4010001

Moudrý V, Klápště P, Fogl M, Gdulová K, Barták V, Urban R (2019) Assessment of LiDAR ground filtering algorithms for determining ground surface of non-natural terrain overgrown with forest and steppe vegetation. Measurement 150, article id 107047. https://doi.org/10.1016/j.measurement.2019.107047
Muir J, Goodwin N, Armston J, Phinn S, Scarth P (2017) An accuracy assessment of derived digital elevation models from terrestrial laser scanning in a sub-tropical forested environment. Remote Sens 9, article id 843. https://doi.org/10.3390/rs9080843
Nelson K, Chasmer L, Hopkinson C (2022) Quantifying lidar elevation accuracy: Parameterization and wavelength selection for optimal ground classifications based on time since fire/disturbance. Remote Sens 14, article id 5080. https://doi.org/10.3390/rs14205080
Ning J, Liu H, Yu W, Deng J, Sun L, Yang G, Wang M, Yu H (2024) Comparison of different models to simulate forest fire spread: A case study. Forests 15, article id 563. https://doi.org/10.3390/f15030563
Nolde M, Plank S, Riedlinger T (2020) An adaptive and extensible system for satellite-based, large scale burnt area monitoring in near-real time. Remote Sens 12, article id 2162. https://doi.org/10.3390/rs12132162
Okyay U, Telling J, Glennie CL, Dietrich WE (2019) Airborne lidar change detection: An overview of Earth sciences applications. Earth Sci Rev 198, article id 102929. https://doi.org/10.1016/j.earscirev.2019.102929
Olsoy PJ, Glenn NF, Clark PE, Derryberry DR (2014) Aboveground total and green biomass of dryland shrub derived from terrestrial laser scanning. ISPRS J Photogramm Remote Sens 88: 166–173. https://doi.org/10.1016/j.isprsjprs.2013.12.006
Or D, Furtak-Cole E, Berli M, Shillito R, Ebrahimian H, Vahdat-Aboueshagh H, McKenna SA (2023) Review of wildfire modeling considering effects on land surfaces. Earth Sci Rev Reviews 245, article id 104569 https://doi.org/10.1016/j.earscirev.2023.104569
Orwig DA, Boucher P, Paynter I, Saenz E, Li Z, Schaaf C (2018) The potential to characterize ecological data with terrestrial laser scanning in Harvard Forest, MA. Interface focus 8, article id 20170044. https://doi.org/10.1098/rsfs.2017.0044
Palviainen M, Finér L, Mannerkoski H, Piirainen S, Starr M (2005) Responses of ground vegetation species to clear-cutting in a boreal forest: Aboveground biomass and nutrient contents during the first 7 years. Ecol Res 20: 652–660. https://doi.org/10.1007/s11284-005-0078-1
Parviainen J (1996) Impact of fire on Finnish forests in the past and today. Silva Fenn 30: 353–359. https://doi.org/10.14214/sf.a9246
Penman S, Lentini P, Law B, York A (2023) An instructional workflow for using terrestrial laser scanning (TLS) to quantify vegetation structure for wildlife studies. For Ecol Manage 548, article id 121405. https://doi.org/10.1016/j.foreco.2023.121405
Penman TD, Kavanagh RP, Binns DL, Melick DR (2007) Patchiness of prescribed burns in dry sclerophyll eucalypt forests in South-eastern Australia. For Ecol Manage 252: 24–32. https://doi.org/10.1016/j.foreco.2007.06.004
Penttilä R, Junninen K, Punttila P, Siitonen J (2013) Effects of forest restoration by fire on polypores depend strongly on time since disturbance – A case study from Finland based on a 23-year monitoring period. For Ecol Manage 319: 508–516. https://doi.org/10.1016/j.foreco.2013.08.061
Pérez-Izquierdo L, Clemmensen KE, Strengbom J, Granath G, Wardle DA, Nilsson M-C, Lindahl BD (2020) Crown-fire severity is more important than ground-fire severity in determining soil fungal community development in the boreal forest. J Ecol 109: 504–518. https://doi.org/10.1111/1365-2745.13529

Perkiö R, Puustonen M, Similä M (2012) Controlled burning to emulate natural forest fires. In: Similä M, Junninen K (eds) Ecological restoration and management in boreal forests – best practices from Finland. Metsähallitus, Vantaa.
Phiri D, Simwanda M, Salekin S, Nyirenda VR, Murayama Y, Ranagalage M (2020) Sentinel-2 data for land cover/use mapping: A review. Remote Sens 12, article id 2291. https://doi.org/10.3390/rs12142291
Pleniou M, Koutsias N (2013) Sensitivity of spectral reflectance values to different burn and vegetation ratios: A multi-scale approach applied in a fire affected area. ISPRS J Photogramm Remote Sens 79: 199–210. https://doi.org/10.1016/j.isprsjprs.2013.02.016
Päätalo M-L (1998) Factors influencing occurrence and impacts of fires in northern European forests. Silva Fenn 32: 185–202. https://doi.org/10.14214/sf.695
Rai N, Ma Q, Poudel KP, Himes A, Meng Q (2024) Evaluating the uncertainties in forest canopy height measurements using ICESat-2 data. J Remote Sens 4, article id 0160. https://doi.org/10.34133/remotesensing.0160
Rogers BM, Soja AJ, Goulden ML, Randerson JT (2015) Influence of tree species on continental differences in boreal fires and climate feedbacks. Nat Geosci 8: 228–234. https://doi.org/10.1038/ngeo2352
Ritter T, Schwarz M, Tockner A, Leisch F, Nothdurft A (2017) Automatic mapping of forest stands based on three-dimensional point clouds derived from terrestrial laser-scanning. Forests 8, article id 265. https://doi.org/10.3390/f8080265
Rosette J, Suárez J, Nelson R, Los S, Cook B, North P (2012) Lidar remote sensing for biomass assessment. In: Fatoyinbo T (ed) Remote sensing of biomass. Principles and applications. InTechOpen, Rijeka, pp 3–26. http://dx.doi.org/10.5772/696
Rossa CG, Veloso R, Fernandes PM (2016) A laboratory-based quantification of the effect of live fuel moisture content on fire spread rate. Int J Wildland Fire 25: 569–573. https://doi.org/10.1071/WF15114
Rowell EM, Seielstad CA, Ottmar RD (2016) Development and validation of fuel height models for terrestrial lidar – RxCADRE 2012. Int J Wildland Fire 25: 38–47. http://dx.doi.org/10.1071/WF14170
Ryan KC (2002) Dynamic interactions between forest structure and fire behavior in boreal ecosystems. Silva Fenn 36: 13–39. https://doi.org/10.14214/sf.548
Ryan M (2019) Geometry essentials for dummies. John Wiley & Sons, Hoboken.
Saucier J–P, Baldwin K, Krestov P, Jorgenson T (2015). Boreal forests. In: Peh KS-H, Corlett RT, Bergeron Y (eds) Routledge handbook of forest ecology. Routledge, London, pp 7–29.
Seidel D, Beyer F, Hertel D, Fleck S, Leuschner C (2011) 3D-laser scanning: A non-destructive method for studying above-ground biomass and growth of juvenile trees. Agric For Meteorol 151: 1305–1311. https://doi.org/10.1016/j.agrformet.2011.05.013
Shorohova E, Kneeshaw D, Kuuluvainen T, Gauthier S (2011) Variability and dynamics of old-growth forests in the circumboreal zone: Implications for conservation, restoration and management. Silva Fenn 45: 785–806. https://doi.org/10.14214/sf.72
Soverel NO, Perrakis DDB, Coops NC (2010) Estimating burn severity from Landsat dNBR and RdNBR indices across western Canada. Remote Sens Environ 114: 1896–1909. https://doi.org/10.1016/j.rse.2010.03.013
Sparks AM, Smith AMS, Hudak AT, Corrao MV, Kremens RL, Keefe RF (2023) Integrating active fire behavior observations and multitemporal airborne laser scanning data to quantify fire impacts on tree growth: A pilot study in mature *Pinus ponderosa* stands. For Ecol Manage 545, article id 121246. https://doi.org/10.1016/j.foreco.2023.121246

Su J, Bork E (2006) Influence of vegetation, slope and lidar sampling angle on DEM accuracy. Photogramm Eng Remote Sens 72: 1265–1274. https://doi.org/10.14358/PERS.72.11.1265

Sun T, Qi J, Huang H (2020) Discovering forest height changes based on spaceborne lidar data of ICESat-1 in 2005 and ICESat-2 in 2019: A case study in the Beijing-Tianjin-Hebei region of China. For Ecosyst 7, article id 53. https://doi.org/10.1186/s40663-020-00265-w

Szpakowski DM, Jensen JLR (2019) A review of the applications of remote sensing in fire ecology. Remote Sens 11, article id 2638. https://doi.org/10.3390/rs11222638

Tanase MA, Pérez-Cabello F, de la Riva J, Santoro M (2010) TerraSAR-X data for burn severity evaluation in Mediterranean forests on sloped terrain. IEEE Trans Geosci Remote Sens 48: 917–929. https://doi.org/10.1109/TGRS.2009.2025943

Thompson I, Mackey B, McNulty S, Mosseler A (2009) Forest resilience, biodiversity, and climate change. A synthesis of the biodiversity/resilience/stability relationship in forest ecosystems. Secretariat of the Convention on Biological Diversity, Montreal.

Tsang L, Durand M, Derksen C, Barros AP, Kang D-H, Lievens H, Marshall H-P, Zhu J, Johnson J, King J, Lemmetyinen J, Sandells M, Rutter N, Siqueira P, Nolin A, Osmanoglu B, Vuyovich C, Kim E, Taylor D, Merkouriadi I, Brucker L, Navari M, Dumont M, Kelly R, Kim RS, Liao T-H, Borah F, Xu X (2022) Review article: Global monitoring of snow water equivalent using high-frequency radar remote sensing. Cryosphere 16: 3531–3573. https://doi.org/10.5194/tc-16-3531-2022

Vanha-Majamaa I, Lindberg H, Heikkilä T (2004) Forest fire research in Finland. Int For Fire News 30: 22–28.

Vauhkonen J, Maltamo M, McRoberts R, Næsset E (2014) Introduction to forestry applications of airborne laser scanning. In: Maltamo M, Næsset E, Vauhkonen J (eds) Forestry applications of airborne laser scanning. Concepts and case studies. Springer, Dordrecht, pp 1–16. http://doi.org/10.1007/978-94-017-8663-8

Veraverbeke S, Lhermitte S, Verstraeten WW, Goossens R (2011) Evaluation of pre/post-fire differenced spectral indices for assessing burn severity in a Mediterranean environment with Landsat Thematic Mapper. Int J Remote Sens 32: 3521–3537. https://doi.org/10.1080/01431161003752430

Wallace L, Gupta V, Reinke K, Jones S (2016) An assessment of pre- and post fire near surface fuel hazard in an Australian dry sclerophyll forest using point cloud data captured using a terrestrial laser scanner. Remote Sens 8, article id 679. http://doi.org/10.3390/rs8080679

Wang Z, Zhang T, Huang X (2023) Predicting real-time fire heat release rate by flame images and deep learning. Proc Conbust Inst 39: 4115–4123. https://doi.org/10.1016/j.proci.2022.07.062

Wittke S, Fouilloux A, Lehti P, Varho J, Kivimäki A, Karhu M, Karjalainen M, Vaaja M, Puttonen E (2023) EODIE – Earth observation data information extractor. SoftwareX 23, article id 101421. https://doi.org/10.1016/j.softx.2023.101421

Wulder MA, Roy DP, Radeloff VC, Loveland TR, Anderson MC, Johnson DM, Healey S, Zhu Z, Scambos TA, Pahlevan N, Hansen M, Gorelick N, Crawford CJ, Masek JG, Hermosilla T, White JC, Belward AS, Schaaf C, Woodcock CE, Huntington JL, Lymburner L, Hostert P, Gao F, Lyapustin A, Pekel J-F, Strobl P, Cook BD (2022) Fifty years of Landsat science and impacts. Remote Sens Environ 280, article id 113195. https://doi.org/10.1016/j.rse.2022.113195

Xiong S, Nilsson C (1999) The effects of plant litter on vegetation: A meta-analysis. J Ecol 87: 984–994. https://doi.org/10.1046/j.1365-2745.1999.00414.x

Yao T, Yang X, Zhao F, Wang Z, Zhang Q, Jupp D, Lovell J, Culvenor D, Newnham G, Ni-Meister W, Schaaf C, Woodcock C, Wang J, Li X, Strahler A (2011) Measuring forest structure and biomass in New England forest stands using Echidna ground-based lidar. Remote Sens Environ 115: 2965–2974. https://doi.org/10.1016/j.rse.2010.03.019

Yebra M, Dennison PE, Chuvieco E, Riaño D, Zylstra P, Hunt Jr ER, Danson FM, Qi Y, Jurdao S (2013) A global review of remote sensing of live fuel moisture content for fire danger assessment: Moving towards operational products. Remote Sens Environ 136: 455–468. https://dx.doi.org/10.1016/j.rse.2013.05.029

Yin C, He B, Yebra M, Quan X, Edwards AC, Liu X, Liao Z (2020) Improving burn severity retrieval by integrating tree canopy cover into radiative transfer model simulation. Remote Sens Environ. 236, article id 111454. https://doi.org/10.1016/j.rse.2019.111454

Yoon H, Song H, Park K (2011) A phase-shift laser scanner based on a time-counting method for high linearity performance. Rec Sci Instrum 82, article id 075108. https://doi-org.ezproxy.uef.fi:2443/10.1063/1.3600456

Yrttimaa T (2021) Automatic point cloud processing tools to characterize trees (PointCloud-Tools: v1.0.1). Zenodo. https://doi.org/10.5281/zenodo.5779288

Yrttimaa T, Saarinen N, Kankare V, Liang X, Hyyppä J, Holopainen M, Vastaranta M (2019) Investigating the feasibility of multi-scan terrestrial laser scanning to characterize tree communities in southern boreal forests. Remote Sens 11, article id 1423. https://doi.org/10.3390/rs11121423

Yrttimaa T, Saarinen N, Kankare V, Hynynen J, Huuskonen S, Holopainen M, Hyyppä J, Vastaranta M (2020) Performance of terrestrial laser scanning to characterize managed Scots pine (*Pinus sylvestris* L.*)* stands is dependent on forest structural variation. ISPRS J Photogramm Remote Sens 168: 277–287. https://doi.org/10.1016/j.isprsjprs.2020.08.017

Zagalikis G (2023) Remote sensing and GIS applications in wildfires. In: Abdalla RM (ed) Geographic information systems – Data science approach. IntechOpen. https://doi.org/10.5772/intechopen.111616

Zhao Y, Liu X, Wang Y, Zheng Z, Zheng S, Zhao D, Bai Y (2021) UAV-based individual shrub aboveground biomass estimation calibrated against terrestrial LiDAR in a shrub-encroached grassland. Int J Appl Earth Obs Geoinf 101, article id 102358. https://doi.org/10.1016/j.jag.2021.102358

Zhao Y, Huang Y, Sun X, Dong G, Li Y, Ma M (2023) Forest fire mapping using multi-source remote sensing data: A case study in Chongqing. Remote Sens 15, article id 2323. https://doi.org/10.3390/rs15092323

Zhu L, Suomalainen J, Liu J, Hyyppä J, Kaartinen H, Haggren H (2017) A review: Remote sensing sensors. In: Rustamov RB, Hasanova S, Zeynalova MH (eds) Multi-purposeful applications of geospatial data. IntechOpen. http://doi.org/10.5772/intechopen.71049